BUKU PROFIL PENYELIDIKAN SKIM GERAN PENYELIDIKAN FUNDAMENTAL (FRGS) FASA 1/2014

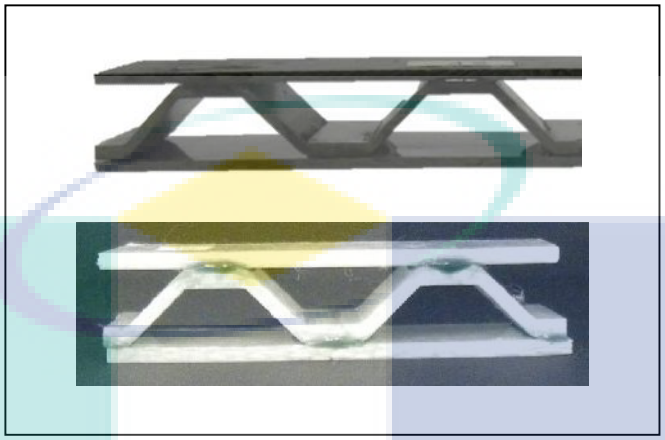

MODELLING OF LIGHTWEIGHT SANDWICH STRUCTURES BASED ON CORRUGATED-CORES

Name of Project Leader: Dr. Mohd Ruzaimi Bin Mat Rejab

Name of co-researchers:

1. Prof. Dr. Md. Mustafizur Rahman
2. Assoc. Prof. Dr. Kumaran Kadirgama
3. Dr. Dandi Bachtiar
4. Dr. Januar Parlaungan Siregar
5. Dr. Ahmad Syahrizan Sulaiman

IPT: Universiti Malaysia Pahang
E-mail: ruzaimi@ump.edu.my
FRGS Field: Mechanical & Manufacturing

ABSTRACT (120 words)

Trapezoidal corrugated-core was fabricated using a 45^{o} profiled mould, and used to form a range of lightweight sandwich structures. The 45^{o} corrugation angle was chosen since it represents an optimal configuration for all combinations of bending and shearing stiffness. The compressive behaviour and failure mechanism in the structures based on two different materials have been investigated experimentally. This research work aims to study the behaviour of trapezoidal corrugated-core subjected to tension and compression stresses, the effect of varying the geometrical parameters on the corrugated-core behaviour and to model the mechanical response of trapezoidal corrugated-core with sandwich structures. Trapezoidal corrugated-cores were made of carbon fibre reinforced plastic (CFRP) and glass fibre reinforced plastic (GFRP). Corrugated composites were designed using conventional manufacturing technique and then bonded to skins using adhesive based on the same material, to produce a range of lightweight sandwich structures. The thickness of the cell walls, number of unit and width cell were used in determining the behaviour of the mechanical structures. The initial failure modes in this corrugated structure are struts buckling, fibre cracking, and delamination in the composite structure. Compression loading was subsequently performed on the trapezoidal corrugated structure, where the compression strength shows increasing for all the corrugation structure. To simulate the mechanical response of the corrugation structure, Finite Element (FE) models were developed using ABAQUS/CAE. The results were compared to measure the experimental outcome. From the finding, the effects of varying the number of unit cell dominate by CFRP are higher than GFRP that 2.08 MPa at three unit cell. It shows that the higher number of unit cells it affects the composite strength. For the effect of cell wall thickness, the results show that the higher the wall thickness, the higher the compression strength. The structures show excellent repeatability in terms of their mechanical response. The mechanical response in compression increases with specimen thickness. For validation between FE result and experimental data, a very good agreement is found between experimental and finite element values. This observation is validated by computing the percentage error between the finite element and the experimental results with average difference around 4.97% in maximum load.

1. INTRODUCTION

The progressive and the use of materials for structural and other design purposes are growing rapidly. One of the most important characteristics in structural studies is reducing the weight without neglecting the strength of a structure. Hence, this engineering challenge has led numerous of researchers to model and fabricate lightweight structures that can give greater strength, and absorb more energy under several loading conditions. Reducing the weight while increasing the strength is always critical, from airliners to future space missions to the Mars. Research in sandwich cores today may lead to radical improvements in the future.

One of the solutions to achieve light weight is by changing metals with composites. A composite is a material having two or more separate components or phases, which are both components, are present in reasonable proportions, each having dissimilar properties, causing in altogether different properties for the composite material produced. The components present in a continuous form and often but not always present in the greater quantity called the 'matrix', such as polymeric materials. In general, polymers are well-known of its poor strength and a low Young's modulus.

The second component is termed as the reinforcing phase or the 'reinforcement', with the purpose of enhancing or reinforcing the mechanical properties of the matrix, such as the carbon fibre. In common, the reinforcement is stronger and stiffer than the matrix.

There has been an increase for more than a half-century in the use of composites and sandwich constructions in a wide range of usages. These applications include structures in the aerospace, automotive, naval and construction industries. For example, the largest airliner in the sky, the Airbus A380, is an outstanding example of the development in the use of the composite materials.

Figure 1.1: Contribution of composite material on A380 Airbus (http://www.malaysiasite.nl/fleet.html)

Figure 1.1 presents the distribution of composite materials in the A380. The increased use of carbon fibre reinforced plastic (CFRP) laminates has resulted in a drastic weight reduction in the A380 (Pora, 2001). The major material improvements in the A380 are its CFRP composite centre wing box, which is the first in commercial aviation. CFRP has also replaced aluminium on the side panels and the secondary rib.

A sandwich structure usually comprises of two thin stiff skins, made from a dense material, and separated by a thick and light core. The outcome of this construction is a structure with a high bending stiffness and strength with a low overall density. Indeed, the bending stiffness and strength of a sandwich structure are always greater to that of a monolithic structure made from the same material and having the same weight.

The skin materials are one of the essential components in sandwich structures. It can be divided into fibre reinforced composites and non-composites. For the non-composites, the most common skin material is an aluminium sheet metal. Its applications include refrigerated transportation containers and construction panels. Most fibre reinforced composites employed as the skins in a sandwich structure. The most common fibres include glass fibre, carbon fibre and aramid. In general, composites skins have an excellent strength, stiffness, corrosion resistance, thermal properties and are lightweight in nature. Nevertheless, composites are bit expensive than sheet metals and sometimes require complex manufacturing processes. The composite skin may comprise of different designs, such as unidirectional (UD), chopped strand mat (CSM) and woven roving (WR). UD skin has high strength in one direction (fibre direction only), whereas a WR skin has moderate strength in two perpendicular directions.

Sandwich structures commonly based on polymeric foam and honeycomb core materials may retain air and humidity. Humidity retention is one of the problems in aeroplane sandwich construction. This problem may lead to an increase in the overall weight of the sandwich structure and degrading of the core properties. To overcome the problems, an open channel core material such as two-dimensional prismatic core is vent-able in order to avoid moisture accumulation. In the development process, characteristics of the mechanical behaviour of the corrugated-core will be studied using the uniaxial loading conditions. The structural models will be constructed using the CAD software and analysed by utilising the finite element (FE) software. The prediction model will be developed for the analysis of corrugated-core sandwich structures based on the strength and weight and compared with the experimental results to predict the strength and failure mechanisms of the corrugated-cores. In addition, the suitability of the corrugated-core as replacement core design structures in the sandwich construction will be as well serves the concept of sustainable manufacturing.

Application of Corrugated-core sandwich structure

In the packaging industry, the corrugated box was initially used for packaging glass and pottery containers. This corrugated box is a paper-based material, consisting of a flute (core) corrugated sheet and one or two flat linerboards. The first corrugated paper design was patented in England in 1856. Today, packaging engineers design and develop corrugated boxes (shipping containers) to satisfy the particular needs of the product being shipped and the hazards of the shipping surroundings, i.e. shock, compression, moisture, vibration.

Corrugated structure in aerospace application was used by several researchers to study morphing wings. Morphing wings can improve aircraft efficiency, by eliminating weight and mechanical systems. The technology requires anisotropic materials, high span-wise stiffness and high chord-wise flexibility. Previous work identifies such materials and this project aims to investigate the deflection behaviour under flight conditions.

The versatility of corrugated structures allows their use not only in the construction of culverts under motor roads and railway lines but also in the construction of overhead crossings, bridleways, pedestrian and transport tunnels and avalanche galleries. In urban and industrial sites, corrugated steel structure is used in the construction of

drainage systems, storm water drains, utility galleries, site landscaping, flood protection structures, water flow regulation, coast establishing and coast protecting structures.

Problem Statement

The most ordinary foams are made from polymers. In general, polymeric foams are suitable as energy absorption devices and heat insulators. Unfortunately, polymeric foams offer a highly irregular cell structure, mostly closed channels and are very conventional. Sandwich structures with closed channel cellular materials may retain air and humidity. Humidity retention is one of the problems in aeroplane sandwich construction. This issue may lead to an increase in the overall weight of the sandwich structure and degrading of the core properties. Traditional sandwich core material such as polymeric foams and honeycomb cores exhibit poor air flow exchange. Therefore, corrugated-core geometries from composite material that has a good strength to weight ratio with an open channel will be studied. The corrugated channel will allow good air flow to remove humidity while composite with trapezoidal geometry will increase the mechanical performance. Thus, the mechanical performance of the corrugated channel will be investigated in this project.

Objective

The main objectives of the project are as follows:

1. To investigate the behaviour of trapezoidal corrugated-core subjected to tension and compression loading.
2. To model with the mechanical response of trapezoidal corrugated-core sandwich structures in Finite Element software.
3. To study the effect of varying the geometrical parameters and properties of the corrugated-cores.

Scope

The scope of work is specified as follows:

1. Development of lightweight sandwich structure based on 45^{o} angle trapezoidal corrugated-core.
2. Carbon fibre reinforced plastic (CFRP) and glass fibre reinforced plastic (GFRP) as investigated materials for the sandwich structure.
3. Static compression and tension tests using Universal Testing Machine.
4. FE modelling of the sandwich structure using ABAQUS/CAE software.
5. The effects of trapezoidal corrugated-core are limited to varying cell wall thickness and number of unit cell.

2. LITERATURE REVIEW

A range of sandwich cores has been manufactured with the objective of developing a lightweight structure, which is both robust and stiff. From balsa wood of the 'mosquito aircraft' to polymer foams and honeycomb cores, and recently more researchers are investigating ideal lightweight cellular core candidates for sandwich structures (Bartolozzi et al., 2013; Côté et al., 2006; Heimbs, 2009; Malcom et al., 2013; Rejab & Cantwell, 2013; Yokozeki et al., 2006). The mechanical properties of sandwich core materials dominated by three factors; the topology of the cellular materials, the properties of the parent and the relative density, ρ* defined by the volume fraction of solid material (Evans et al., 2001).

Cellular materials exhibit desirable qualities, such as low density, high strength, high stiffness and high energy absorption. With careful design, these qualities can be combined as multifunctional components (Evans et al., 2001). The potential for cellular materials to have a multifunctional performance makes them even more attractive to researchers. For examples, fold-cores feature multifunctional properties, such as thermal insulation and good acoustic damping, in addition to their mechanical properties (Abbadi et al., 2009). Furthermore, the problem of humidity accumulation in closed-cell sandwich core materials such as honeycomb can be solved. In general, the open cell design of prismatic, truss and textile cores permits vent ability, resulting in improves of air flow.

The manufacture of strong and stiff cellular materials requires the correct selection of materials and topologies. An appropriate combination can delay the onset of failure modes such as yielding or plastic buckling in metals, and delamination or fibre fracture in fibre fracture in fibre reinforced composites. Since the majority of studies in the field of sandwich structures are of polymeric and honeycomb core materials, there is very few information in the open literature on corrugated-cores. Optimisation of shape design will be conducted and corrugated-core sandwich structure will be performed, and the simulation results will be validated against the experimental data.

Sandwich Structure

The sandwich structure comprises of two relatively thin, stiff and strong faces separated by a relatively thick lightweight core, for example, honeycomb, foam core and cellular metal. Stiff and simultaneous light component is crucial in industries nowadays. To achieve lightweight and high stiffness component, sandwich structure construction was developed (Belouettar et al., 2009; Burlayenko & Sadowski, 2009; Grujicic et al., 2013; Petras & Sutcliffe, 1999)

Depending on the purpose of the materials can differ; nevertheless, the most important characteristics for sandwich structures are, they are lightweight compared to metallic, high stiffness and cost-effective compared to other composite structures. For specific applications using core material such as in aerospace, automotive, marine transportation, satellites, truck structures, containers, tanks, body parts, rail cars and wind energy systems, the production technology used for the sandwich structure is significant (Belouettar et al., 2009, and Burman & Zenkert, 1997).

Sandwich structures are being considered for application regarding aircraft main structures, where durability and damage tolerance is a first rank consideration, thus, understanding the adverse effect of in-service events. In fact, development of the composite structure to sensitive fields, where high reliability is required, such as civil flight, was so far limited by the poor knowledge of their behaviour under multiple dynamic loads. So, the structure needs to be assessed to verify that damage occurring during the service life will not lead to failure or extreme structural deformation until the

damage is detected. The knowledge of their static and fatigue behaviour are required to use the material in a different application, and a better considerate of the numerous failure mechanisms under static and fatigue loadings situations is essential and extremely necessary (Belouettar et al., 2009).

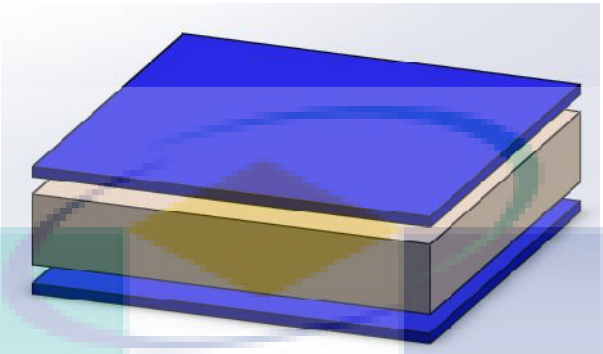

Figure 2.1: Example of foam core sandwich structure (Konka et al., 2012)

Because of their high specific strengths and stiffness, sandwich structures are extensively used in lightweight construction especially aerospace industries (Dayyani et al., 2002; Mohammadi et al., 2015; Mohan et al., 2011). Figure 2.1 shows the example of foam core sandwich structure. Sandwich panel comprises a lightweight core covered by two thin face sheets. Every face sheet may be an isotropic material or a fibre-reinforced composite laminate while the core material may either be of metallic/polymeric foam or metallic/aramid honeycomb (Foo et al., 2007). The main profits of using the sandwich concept in structural components are the high stiffness and low weight ratios. These structures can carry in-plane and out-of-plane loads and show good steadiness under compression, keeping the excellent strength to weight and stiffness to weight characteristics. There are many advantages of sandwich constructions, the expansion of new materials and the need for high performance and low-weight structures ensure that sandwich construction will continue to be in demand (Belouettar et al., 2009, and He & Hu 2008).

The core is made up of polymers, wood, aluminium and composites. These are to minimize its weight that are used in form of foams, corrugated and honeycombs construction (Petras & Sutcliffe 1999).

Sandwich structures with cellular core materials compromise high definite strength and an interest energy absorbing capacity. Such sandwich structure properties make them a good solution for the protection of aircraft structure from impacting unknown objects. For example, such panels are frequently used in front of airplane to avoid accidental bird strikes, which can cause major damages to equipment and thus affect their safety. This protection is to avoid damage of panels which can cause the depressurization of aircraft (Zhao et al., 2007).

Sandwich concept is a proven construction technique that combines low weight with exceptionally high strength thereby making it ideal for a wide range of applications in the aerospace, marine, wind energy and transportation industries (Belingardi et al., 2007; Ivañez et al., 2010).

In principle, a sandwich consists of two faceplates (facings or faces), which are comparatively thin but of high strength and stiffness, enclosing a core structure, which is relatively thick but lightweight, and possesses sufficient stiffness in the direction

normal to the plane of the face plates. The components of the sandwich material are bonded together, using either adhesives or mechanical fastenings, such that they can act as a composite load-bearing unit. The skins withstand the bending stresses and give the structure a hardwearing surface whereas light core material carries the shear stresses generated by loads, distributing them over a larger area. Combining together different materials and geometries, it is possible to obtain a wide range of structures and therefore to reach a great flexibility of use (Belingardi et al., 2007).

Type of Sandwich Structures

In current years, there are several types of sandwich structures with better quasi-static and dynamic properties have been introduced, comprising those based on various foam, honeycomb cores, truss cores and origami cores (Rejab & Cantwell, 2013).

Honeycomb Sandwich Structure

Honeycomb is well-known core used to build sandwich structure. The name comes from the structure of honeycombs made by bees to store honey. Honeycombs and flex cores are used in many applications, for example chassis of modern Formula One cars. The honeycomb, Flex cores and Nomex are sandwiched between two carbon skins with the purpose of making a very stiff and strong structure that offers shield to the driver in case of a simple crash.

In aerospace applications, honeycomb materials have been used broadly among core materials. Various studies have been conducted to understand the mechanical response of honeycomb structures under dissimilar loadings (Aktay et al., 2008).

Normally honeycomb has a uniform shape of hexagonal structure defined by the cell size, material, cell wall thickness and bulk density. The main constructional materials are glass fibre reinforced plastic, aluminium and aramid paper. Among them, aramid paper and aluminium are usually used in engineering application. While aluminium honeycomb sandwich structures are structurally efficient, their use in the aerospace industry is now limited due to a susceptibility to long-term moisture exposure which leads to corrosion, degradation of the adhesive bonds and extensive face sheet debonding (Choi & Jang, 2010; Li, Ueno, & Lefebvre, 2006; Saarimäki & Ylinen, 2008). This degradation has caused a number of in-flight failures, failure of panels during repair and an increased maintenance burden in assessing and repairing damage. (Aktay et al., 2008).

Honeycombs are produced by bonding metal or composite laminate skins to a honeycomb core. These layered-like materials are characterized by lightweight, high flexural stiffness and can support classical loadings like tension and bending. The advantages of honeycomb sandwich constructions together with the development of new materials and the industrial needs for high performance and low-weight structures ensure that honeycomb sandwich construction will continue to be in demand. Honeycomb composites are increasingly being used to replace traditional materials in highly loaded applications. Honeycomb cores are described as cellular solids that make use of voids to decrease mass, while maintaining qualities of stiffness and energy absorption. This improvement, at relatively little expense, in terms of mass, is of great interest in aerospace, automotive and many other applications. In order to use these materials in different applications, the knowledge of their mechanical behaviour is required. This calls for the development of rigorous mathematical and experimental methods capable of characterizing, modelling, designing and optimizing of the composite under any given set of conditions (Abbadi et al., 2009).

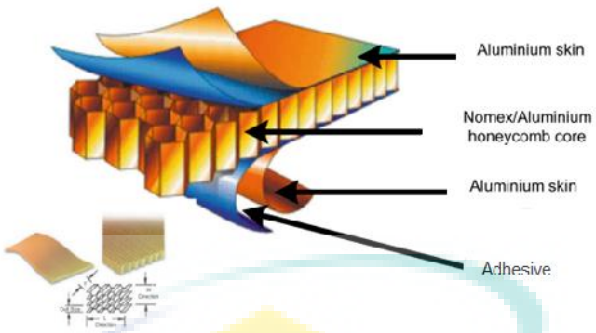

Figure 2.2: Example of Honeycomb sandwich structure (Abbadi et al., 2009)

Figure 2.2 shows an example of honeycomb sandwich structure. A typical honeycomb sandwich panel consists of two thin and stiff facing materials bonded to a thick and lightweight thin-walled core with in-plane two-dimension periodic cellular structure (Frank Xu & Qiao, 2002).

Conventional hexagonal honeycomb sandwiches have been widely applied in aerospace industry since 1940s. With the development of composite materials and manufacturing technology, the application of this efficient structure has been penetrating into every possible field. Circumstantially, honeycomb sandwiches can be optimized from geometry to material in both global and local levels. Among them, one important choice is of honeycomb cores, where the size, shape, topology and wall thickness of core configuration and constituent materials can be comprehensively optimized by taking account of local interactions and consequent global behaviours (Frank Xu & Qiao, 2002).

Honeycomb sandwich structure combines high flexural rigidity and bending strength with low weight (He & Hu, 2008). Honeycomb sandwich materials are being used widely in weight sensitive and damping structures where high flexural rigidity is required, in many fields especially in the automobile industry. Honeycomb core sandwich panel is formed by adhering two high-rigidity thin-face sheets with a low-density honeycomb core possessing less strength and stiffness. By varying the core and the thickness and material of the face sheet, it is possible to obtain various properties and desired performance, particularly high strength-to-weight ratio (He & Hu 2008).

Honeycomb structures have been received much attention in recent years because of their high strength/weight and stiffness/weight ratios, excellent heat resistance and favourable energy-absorbing capacity. Of the various materials used in honeycomb cells, aluminium honeycomb structures have been widely adopted in the aerospace, electronics and architectural industries. Sandwich plates that are manufactured by bonding the skin plates on a honeycomb core using adhesives have been extensively developed to extend the range of applications of honeycomb cells (Jen & Chang, 2008). This study analysed the four-point bending fatigue strengths of aluminium honeycomb sandwich beams with cores of various relative densities. The debonding of the adhesive between the face sheet and the core was identified to be the major failure mode (Jen & Chang, 2008).

Extensive applications of hexagonal honeycomb cores are found particularly in the aerospace and naval industries. In view of the recent interest in novel strong and lightweight core architectures, square honeycomb cores were manufactured and tested under uniform lateral compression (Rejab et al., 2014).

Nomex honeycomb is made from Nomex paper, which is a form of paper made of aromatic polyamide (aramid) fibres. The initial paper honeycomb is usually dipped in a phenolic resin to produce a honeycomb core with high strength and very good in term of fire resistance (Foo et al., 2007). Nomex, the core which this focuses on, is a widely used honeycomb material manufactured by dipping a paper honeycomb substrate into phenolic resin to build up the walls of the honeycomb. As well as mechanical requirements, core materials may also be selected based on their fire resistance or thermal properties (Petras & Sutcliffe 1999).

***Foam** Core Sandwich Structure*

Numerous core materials and core configurations have been offered nowadays. The most generally used core materials are honeycomb and foams. The foam cores are first used when the waterproof, sound and heat insulation qualities of cores are essential. Moreover, the foam cores are the least expensive among core materials and it can give some advantages in sandwich fabrication (Burlayenko & Sadowski, 2009; George et al., 2014; Xu et al., 2016)

Filling the foam in honeycomb cells can be considered as the improvement of debonding resistance and ability to produce new types of sandwich cores. This concept combines the benefits of honeycomb and foam cores. The increased adhesive area of foam-filled honeycomb cells is only one of them. In contrast, the filling leads to changes of the dynamic properties of the honeycomb sandwiches (Burlayenko & Sadowski, 2009).

Moderate reduction of the magnitudes of the natural frequencies causes by introduction of the foam in the honeycomb core. This outcome is magnified by the density of foam fillers, which also insignificantly increases the stiffness and total mass of the filled sandwich plates. Filling of the honeycomb with the foam promotes the slight increases of buckling loads and the insignificant decreases of imperfection sensitivity of foam-filled sandwich plates. Alternatively, adding the foam can induce changes in stress distributions in the core to sheet faces interface. (Bin et al., 2015; Burlayenko & Sadowski, 2009; Yan et al., 2014; Yazici et al., 2014).

The use of cellular foams as a structural element and load bearing component has increased as sandwich constructions become more widely used. Today, the main effort in design is put into face materials, but as the demands for more optimized structures are raised, the research in the field of core materials also increases (Burman & Zenkert 1997). Styles et al., 2007 investigated the effect of core thickness on the deformation mechanism of an aluminium foam core/thermoplastic composite facing sandwich structure under 4 point bending with varying core thicknesses. Kesler & Gibson, 2002 studied size effects in metallic foam core sandwich beams. This is the most substantial effect for the design of sandwich panel with metallic foam core, in which the core is loaded primarily in shear.

Plastic collapse modes of sandwich beams have been studied experimentally and theoretically for the case of aluminium alloy foam with cold-worked aluminium face sheets. Plastic collapse is divided into three competing mechanisms: face yield, indentation and core shear, with the active mechanism depending upon the choice of geometry and material properties (Chen et al., 2001). Rizov, 2006 investigated the elastic-plastic behaviour of closed-cell cellular foams subjected to point and line loads, both experimentally and numerically.

Previously, Chen et al., 2001 explained that a range of metal foams have been established with a relative density ρ (defined by the ratio of foam density to the density of the cell walls) in the range 0.05 to 0.3. Generally are based on aluminium alloys,

though steel foams and creep-resistant nickel alloy foams are also under progress. Metal foams compete favourably with polymer foams as the lightweight cores of sandwich beams, plates and shells, due to the higher stiffness and high-temperature ability.

In this investigation, sandwich beams have been fabricated with an Alporas aluminium alloy foam core, and cold-rolled aluminium face sheets in the half hard condition. The monotonic failure response of the beams has been measured for a wide range of geometries, under four-point bend loading. Four-point bend loading allows the competing failure modes of face yield, core shear and indentation to be separated physically along the beam: face yield occurs between the inner rollers, core shear occurs between the inner and outer rollers and indentation is triggered directly beneath the rollers (Chen et al., 2001).

Aluminium foam sandwiches (AFS) obtained by combining metal face sheets with a lightweight metal foam core, have peculiar properties (low specific weight, efficient capacity of energy dissipation, high impact strength, acoustic and thermal insulation, high damping, etc.), that made them interesting for a number of practical applications, such as the realization of lightweight structures with high mechanical strength and good capacity of energy dissipation under impacts. When compared to traditional honeycomb panels, AFS offer several advantages. They can be made into curved shapes and with integral skins (without adhesive bonding), allowing higher working temperature and higher resistance to damage from water intrusion, which could be important for marine applications (Crupi & Montanini, 2007).

Formerly, the most widely used foamed alloys are aluminium casting alloys due to their relatively low melting temperature, good foamability and low density. Aluminium foams have potential to replace polymer foams in sandwich panel applications due to their increased specific stiffness and higher temperature capability (Harte et al., 2001).

Corrugated-core Sandwich Structure

A corrugated-core sandwich plate comprises of a corrugated sheet between two thin face sheets (Zhang et al., 2015). The significant feature of this structure is its high strength-to-weight ratio. The corrugated-core keeps the face sheets apart and stabilizes them by resisting vertical deformations, and also enables the whole structure to act as a single thick plate as a virtue of its shearing strength. This second feature imparts outstanding strength to the sandwich structures. In addition, unlike soft honeycomb-shaped cores, a corrugated-core resists bending and twisting in addition to vertical shear. Therefore, corrugated-core sandwich panels, due to their exceptionally high flexural stiffness-to-weight ratio are commonly used in aviation, aerospace, civil engineering and other applications, where weight is an important design issue. This construction approach to form a sandwich plate might be defined as ‘structurally composite’, since its behaviour characteristics are defined by the composite action of its components (Chang et al., 2005).

Corrugated-cores with metal sandwich panels are an attractive industrial solution as structural components thanks to their high stiffness-to-mass ratio. However, using detailed finite element models for numerical computation of their properties leads to large models and long solution time, especially for acoustic simulations. Consequently, reduction of the complex shaped core to an equivalent homogeneous material is commonly used (Bartolozzi et al., 2013).

Among all sandwich structures, corrugated-core structures are an exciting alternative that is being progressively used in the transportation industry. These panels provide different core shapes, such as truss-type corrugations (i.e. triangular), trapezoidal

cores or circular shape (Bartolozzi et al., 2013). Corrugated metal sandwich cores is proven in excellent shock resistant properties, mainly due to their high longitudinal stretching and shear strength (Kazemahvazi et al., 2007).

Trapezoidal Core

Thill et al., 2010 investigated about trapezoidal corrugated aramid/epoxy laminates under huge tensile displacements transverse to the corrugation direction. Static and cyclic experimental testing identified three stages of behaviour in the structure's stress versus global strain response. The common displacement comes from the second stage. This was attributed to the aramid fibre compressive properties and delamination in the corrugated unit cell corner region. This local phenomenon is comparable to a pseudo-plastic hinge that allows large deformations over relatively constant stress levels. This behaviour is thought not to occur in glass and carbon fibre corrugated laminates because it was related specifically to the aramid fibre response. The analytical and numerical analysis shows that the equivalent transverse tensile elastic modulus of the corrugated laminate can be predicted; while the complete three-stage behaviour can also be modelled using non-linear finite element analysis with local elastic-plastic material definitions.

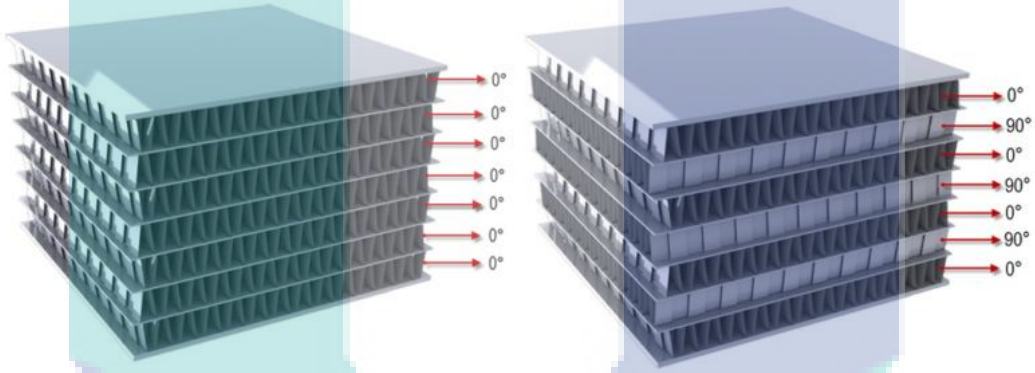

Figure 2.3: Impact Respond of stacked trapezoidal corrugated aluminium core and aluminium sheet interlayer structure (Kiliçaslan et al., 2013)

The finite element modelling (FEM) and the impact responses of stacked trapezoidal corrugated aluminium core and aluminium sheet interlayer sandwich structures was studied by Kiliçaslan et al, 2013. Figure 2.3 shows stacked trapezoidal corrugated aluminium core and aluminium sheet interlayer structure. The simulation and experimental force values were shown to reasonably agree with each other at the large extent of deformation and to reveal the progressive fin folding of corrugated core layers and bending of interlayer sheets as the main deformation mechanisms. The experimentally and numerically determined impact velocity sensitivity of the tested panels was attributed to the micro inertial effects which increased the critical buckling loads of fin layers at increasingly high loading rates.

Experimental and numerical studies on multi-layered corrugated sandwich panels under crushing loading were studied by Hou et al., 2015. In this research, the structures fabricated from trapezoidal aluminium cores and aluminium alloy sheets. It was found that the sandwich configuration and a number of layers played an important role in the failure mechanism and energy absorption Hou et al., 2015. Hou et al., 2013 studied crashworthiness optimization of corrugated sandwich panels based on the trapezoidal and triangular core. W. He et al., 2016 experimented on the low-velocity impact behaviour of hybrid corrugated core sandwich structures together with the numerical research. The core is fabricated with carbon fibre reinforced plastic (CFRP) face sheets and aluminium alloy cores.

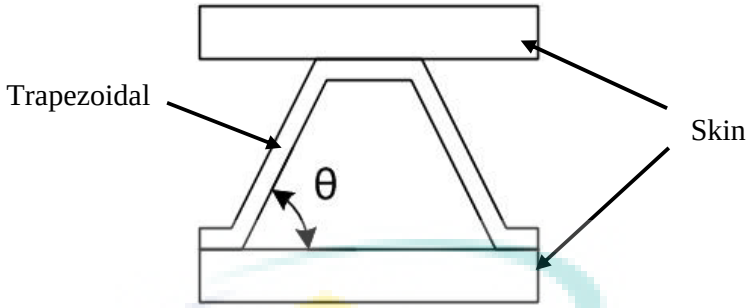

Figure 2.4: Trapezoidal corrugated-core (Bartolozzi et al, 2014)

Kiliçaslan et al., 2014 performed numerical studies and experimental on the quasi-static and dynamic crushing responses of multilayer trapezoidal aluminium corrugated sandwiches. The experimental and simulation compression stress-strain curves show reasonable agreements with each other. Two main crushing modes were observed experimentally and numerically: the progressive fin folding and the shearing interlayer aluminium sheets. Both, the simulation and experimental buckling and post-buckling stresses increased when the interlayer sheets were constraint laterally. The multi-layer samples without interlayer sheets in $0^o/90^o$ core orientation exhibited higher buckling stresses than the samples in $0^o/0^o$ core orientation. The increased buckling stress of $0^o/0^o$ oriented core samples without interlayer sheets at high strain rate was attributed to the micro-inertial effects which led to increased bending forces at higher impact velocities. Figure 2.4 shows an example of trapezoidal corrugated-core with two skins at the upper and bottom of the trapezoidal.

Triangular Core

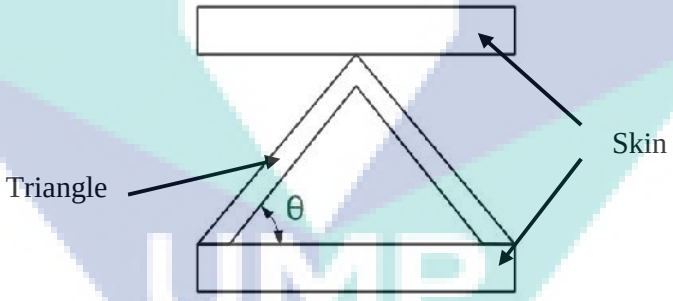

Figure 2.5:Triangular corrugated-core (Bartolozzi et al., 2014)

For triangular shaped corrugated-core, several authors already discussed the strength and properties. For example, (Buannic et al., 2003) studies the homogenization of corrugated sandwich panels. In the studies, several shapes of corrugated-cores were selected including triangular shaped. Rejab & Cantwell, 2013 conducted a series of experimental investigations and numerical analysis, then presented into the compression response, and subsequent failure modes in corrugated-core sandwich panels based on an aluminium alloy, a glass fibre (GFRP) and a carbon fibre reinforced plastic (CFRP). Tian & Lu, 2005 experimented the compression panel consist of different type of corrugated-core including triangular. Figure 2.5 shows an example of triangle corrugated-core with two skins at the upper and bottom of the triangle.

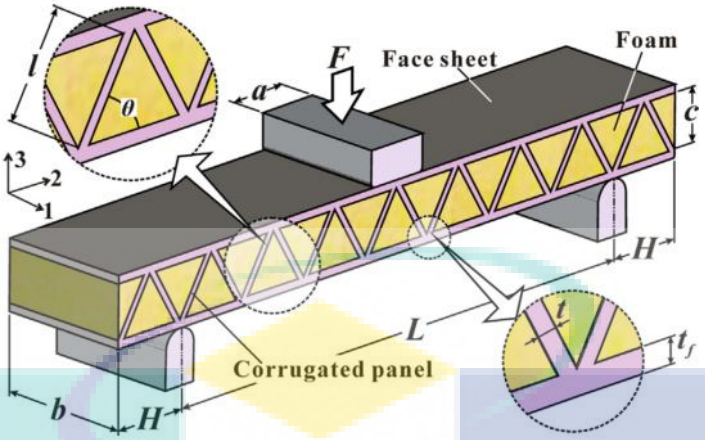

Figure 2.6: Foam filled corrugated sandwich beam (Han et al., 2015)

Numerical and analytical study is carried out by Han et al., 2015 to study the structural stiffness, collapse strength and minimum mass design of foam-filled corrugated sandwich beams under transverse three-point bending. Figure 2.6 shows foam filled corrugated sandwich beam. The structural efficiency of foam filling to reinforced the sandwich is assessed on the basis of equal mass and the underlying mechanisms discovered. It is shown that polymer foam-filled corrugations are more weight efficient than unfilled ones of equal mass.

Sinusoidal Core

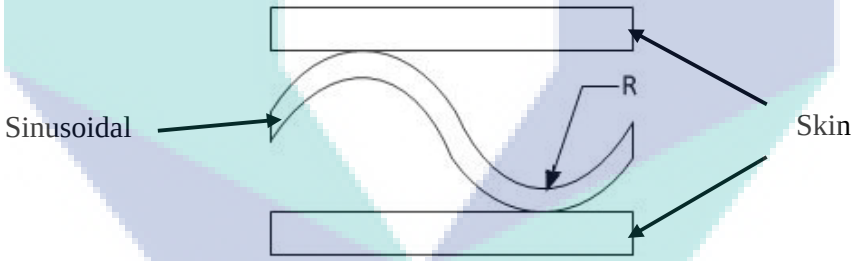

Figure 2.7: Sinusoidal corrugated-core (Bartolozzi et al., 2014)

Bartolozzi et al., 2014 investigated aluminium sandwich panels with sinusoidal corrugated cores as shown in Figure 2.7. The main field of application of these innovative aluminium structures is the transportation sector, e.g. in the automotive industry, where energy conservation, lightweight construction and recycling are critical requirements. Also, marine interior applications are common, since these panels provide good structural performance with small thicknesses plus they can also be easily supplied in semi-finished components. In their research, an innovative aluminium sandwich panel with sinusoidal corrugated core is investigated. The properties of the equivalent material are determined both analytically and numerically for the chosen Reissner–Mindlin orthotropic representation. The two derived models are compared in a comprehensive parametric study to validate computationally with much cheaper analytical formulation. Moreover, a validation of the equivalent models is done based on the bending stiffness per unit width of the sandwich panel. Finally, the acoustic behaviour of the structure is investigated comparing the reduced layered model with the fully detailed 3D model.

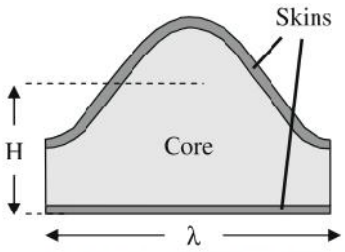

Figure 2.8: Sinusoidal corrugated panel (Reany & Grenestedt, 2009)

Sandwich panel with one corrugated and one flat skin were investigated numerically by Reany & Grenestedt, 2009 with the goal to find configurations with higher strength and/or stiffness and reduced weight. Numerical analyses of the sandwich panels estimated the panel with a corrugated inner skin to be 25% stronger than the conventional panel. The weighing panels indicate that the corrugated panels were 15% lighter than their conventional flat counterparts. Figure 2.8 displays the sinusoidal corrugated panel.

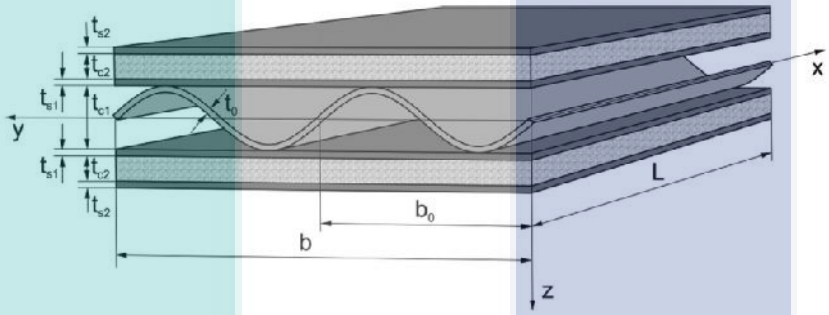

Figure 2.9: Seven layers thin-walled beam (Magnucki et al., 2014)

Magnucki et al., 2014 researched elastic bending and buckling of the seven-layer steel composite beam with transverse sinusoidal corrugated main core and two sandwich faces with steel foam cores. Figure 2.9 shows seven layers thin-walled beam designed by Magnucki et al., 2014.

Isaksson et al., 2007 analysed shear correction factor for corrugated-core structures using sinusoidal corrugated board. The ability of the model to properly capture and simulate the mechanical behaviour of corrugated boards subjected to plate bending as well as three-point bending has been established by means of several numerical examples, which are compared to experiments on corrugated board panels of varying geometry.

Mechanical Performance on Sandwich Structure

Compression Testing on Sandwich Structure

The mechanical characteristics and failure criteria can be studied using compression testing. The compression strength of the material can be investigated through the test. Composite material is designed for upper wing skins of an aircraft where compression strength is a critical application.

Tian & Lu, 2005 investigated the optimal design for corrugated-core panels. Eight different geometry panels are studied, including triangular, hat and blade-stiffened panels, square and trapezoidal cores. Uniform uniaxial compression load test was conducted and calculated by using optimization technique based on sequential quadratic programming (SQP) algorithm. Failure criteria of panels with different cross-

sectional shapes were analysed. The most efficient given boundary condition from a weight viewpoint is about 40% lighter at some load levels than the least efficient-sandwich panels with a square core.

The compressive response of carbon fibre reinforced composite (CFRC) lattice truss sandwich panels (LTSP) was investigated by Hu et al., 2016. Compression and shearing experiments were carried out to reveal the strength and failure modes of the CFRC structure. In this study, a novel corrugated lattice truss sandwich panel reinforced carbon fibre was designed and fabricated. Implementing corrugated topology, the lattice truss panel has much higher shear strength due to significant enlarged node area (Hu et al., 2016).

C. He et al., 2015 discussed the simulated effect on the mechanical properties of bionic integrated honeycomb plates by investigating the compressive and shear failure modes and the mechanical properties of trabeculae reinforced by long or short fibre. An analytical model was proposed for the prediction of face wrinkling behaviour of corrugated-core sandwich columns under dynamic compressive loading perpendicular-to- corrugations (Lim & Bart-Smith, 2015). It was revealed that the dynamic face wrinkling response was also affected by overall column length and the rate of loading unlike the face wrinkling strength of corrugated core sandwich columns in quasi-static compression.

Lim & Bart-Smith, 2016 investigated high-velocity compressive response of metallic corrugated-core sandwich columns. In this investigation, the dynamic response of corrugated-core sandwich columns under high velocities is numerically studied via FEM to gain vision on the dynamic in-plane response. In detailed, the effects of applied velocity and sandwich column geometric dimensions on reaction force are observed. The high-velocity response of corrugated-core sandwich columns compressed parallel to corrugations is also well characterized by the logical expressions based on the theory of wave propagation (Lim & Bart-Smith, 2016).

Che et al., 2014 designed and manufactured octahedral composite sandwich panels by combining upper and lower skins with stitched core to overcome the weak interface between the core and skins of the sandwich structures. Quasi-static compression and shear tests were conducted to get stress-strain curves and to reveal the failure mechanisms of the structure. The octahedral stitched composite cores showed higher specific shear stiffness/strength and out-of-plane compressive strength than conventional sandwich cores, but lower compressive stiffness.

Tensile Testing on Sandwich Structure

As part of a wider study to compare the stiffness properties of corrugated laminates made from different materials and geometries, different experimental results were obtained with trapezoidal corrugated aramid/epoxy laminates subjected to large tensile deformations transverse to the corrugation direction. This study investigates the local failure mechanisms of these specimens that explain the experimental results obtained (Thill et al., 2010). This is carried out via experimental, analytical and numerical analysis methods focusing particularly on the local failure mechanisms and the material behaviour around the corner region of the corrugated unit cell (Thill et al., 2010).

An analytical equivalent model for the mechanical properties of the trapezoidal corrugated core is presented. A complete set of analytical formulations is derive based on energy approach for elastic modulus in different directions, transverse and in-plane shear modulus, in-plane Poisson's ratio and mass density of the equivalent model. A set of tensile and three-point bending tests are also carried out to further evaluate the

derived equations. The results indicate that the analytical relations are accurate for a wide range of geometrical parameters (Mohammadi et al., 2015).

The corrugated composites manufactured from carbon fibre plain woven fabrics draw attention as a candidate material for flexible structural components, e.g. morphing wings. In-plane stiffness and strength of the original corrugated composites are evaluated through the tensile and bending tests in both in-plane longitudinal and transverse directions. A simple analytical model for the initial stiffness of the corrugated composites was developed, and the predictions are compared with the experimental results (Yokozeki et al., 2006).

Numerical Analysis

This section describes the background of the finite element method, the modelling of corrugated-core sandwich structures and other issues involved in static FE modelling.

Finite Element Analysis on Sandwich Structure

The accuracy of the formulation in predicting the equivalent mechanical parameters for the core has been proven by means of FE simulations. Nevertheless, FE models are typically built modelling structures based on some, or even strict, hypotheses. Therefore, to prove the modelling to be the representative of the real sandwich structure behaviour, an experimental is needed (Bartolozzi et al., 2015). The FE models to be validated are built using a multi-layer description in Nastran by means of the PCOMP card, which allows defining layers of different materials, thickness and/or orientation. This information is then used by the software to compute, assuming perfect bonding between layers, an equivalent shell property. Three layers are considered to represent the two skins and the equivalent layer for the core. The FE mesh is properly built to have nodes in correspondence of the measurement points of the panel. The first 15 modes are then computed by the standard Lanczos method. (Bartolozzi et al., 2015)

Kiliçaslan et al., 2014 used FE (Finite Element) to validate with experimental data on quasi-static and dynamic crushing responses of multi-layer trapezoidal aluminium corrugated sandwich. Full geometrical model simulations of quasi-static and dynamic tests were implemented in the non-linear explicit finite element code of LS-DYNA. Trapezoidal corrugated fin layers were meshed using Belytschko–Tsay shell elements with five integration points while the interlayer and face sheets were modelled using constant stress solid elements. Quasi-static simulations were performed at the strain rate of 10^{-1} s^{-1} in order to reduce CPU time. The experimental and simulation compression stress-strain curves showed reasonable agreements with each other. Two main crushing modes were observed experimentally and numerically: the progressive fin folding and the shearing interlayer aluminium sheets. Both of the simulation and experimental buckling and post-buckling stresses increased when the interlayer sheets were constraint laterally.

Yan et al., 2013 studies compressive strength and energy absorption of sandwich panels with aluminium foam-filled corrugated cores. Finite element simulations of both empty and Al foam-filled corrugated panels under quasi-static compression were performed using ABAQUS/Explicit. The geometrical parameters were the same as those of the experimental specimens. The face sheets were modelled as rigid bodies since they are much stiffer than the core structures. Both of the corrugated core members and the filled foam meshed as plane strain elements (i.e., Element CPE4R in ABAQUS). An average element size of 1/10 of the thickness of the corrugated core member was employed for both of the core member and the foam. A mesh size sensitivity study was conducted, revealing that further refining of the mesh had little influence on the numerical results. The face sheets, the core members, and the foam

were assumed to be perfectly bonded together. In general, geometrical imperfections were inevitable in sandwich structures with lattice cores such as corrugated core and truss core. However, due to the low length-thickness ratio of the core member studied here, a very good agreement between the experimental and FE results (assuming perfect bonding) was achieved even without considering any geometrical imperfections. Therefore, the influence of geometrical imperfections was neglected in the present study.

Numerical investigation was conducted by Magnucka-blandzi et al., 2015 to study the mathematical modelling of a transverse shearing effect for sandwich beams with sinusoidal corrugated-cores. The research includes the crosswise corrugated core of beams, the lengthwise corrugated core of beams, the three-point bending problem, the global buckling problem and the influence of a transverse shearing effect. The study includes bending and buckling problems of two sandwich beams, analytical studies have been verified numerically using ABAQUS software (Magnucka-blandzi et al., 2015). Analysis with the buckling and post-buckling behaviour of CFRP cylindrical shells under axial compression using three different types of finite element analyses: eigenvalue analysis, non-linear Riks method and dynamic analysis conducted by Bisagni, 2000.

Simulations of the indentation tests were performed using the commercial finite element analysis software Abaqus/Explicit by McElroy et al., 2015. The purpose of the analysis were to compare results from the indentation experiments to several finite element damage modelling techniques and to investigate what modelling structures are necessary and which are unimportant for a delamination migration simulation.

The response of sandwich steel beams with corrugated cores to quasi-static loading is investigated by employing experimental and computational approaches (Vaidya et al., 2015). The model was meshed with C3D8I elements. The C3D8I element is the first-order fully integrated three dimensional eight nodes solid element, enhanced by incompatible modes to improve its bending behaviour.

3. RESEARCH METHODOLOGY

This section focused on the experimental setup used in this study to investigate the mechanical properties of the corrugated sandwich structure. The test methods used in this study are tensile test and compression test. Tests were conducted on two types of composite materials; carbon fibre reinforced plastic (CFRP) and glass fibre reinforced plastic (GFRP). This study starts with experimental setup for sample preparation. Sample preparation for tensile test is prepared according to Standard test method for tensile properties of polymer matrix composite materials. The materials and fabrication procedures used in this research are also given in this chapter.

Design of mould

The mould was prepared using a 45^{o} trapezoidal corrugated-core profile with a 210 mm by 290 mm effective area of fabrication. It was drawn using Solidwork software before fabricated.

Figure 3.1 shows schematic diagram of trapezoidal corrugated-core with the dimension. Figure 3.2(a) is the Solidwork drawing with upper profile and lower profile and material is in between the profiles. Figure 3.2(b) shows trapezoidal corrugated mould which was fabricated from mild steel. Every unit cell has an average height of 10 mm and a length of 30 mm. The cores used the corrugated 45^{o} profile, as the female mould (lower profile) to hold the composite and as the male mould (top profile) pressed the material to form the shape of a trapezoidal profile.

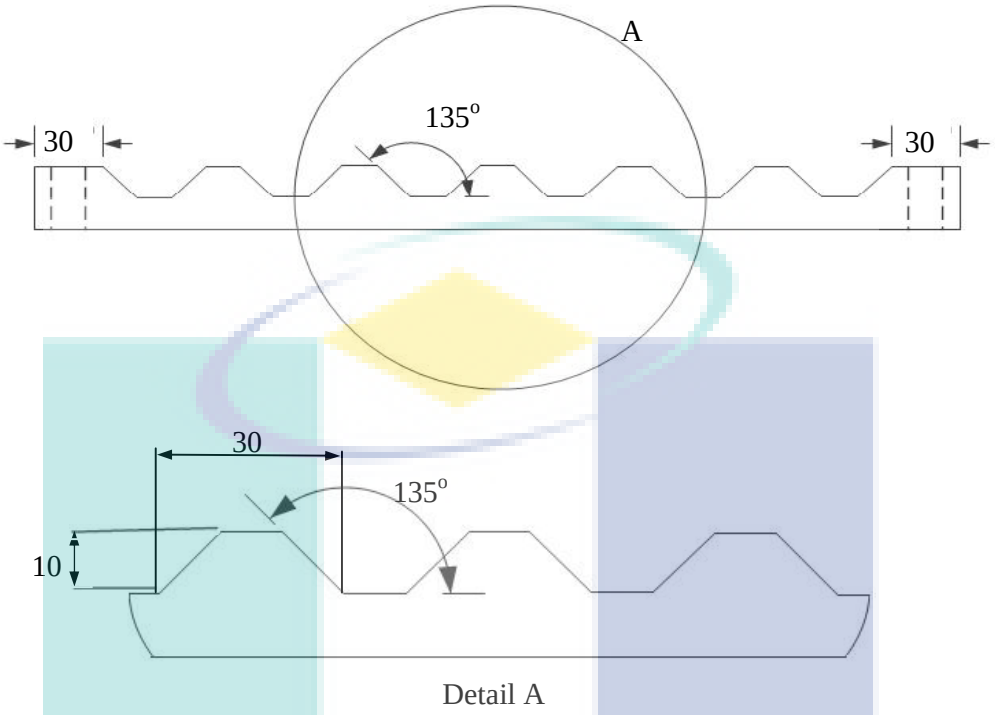

Figure 3.1: Trapezoidal corrugated-core mould with 45° angle

The mould was fabricated using Computer numerical control (CNC) milling machine. Detail A 45° profile was chosen since it gives an optimum shear based on tensile and bending stiffness of core structure (Kazemahvazi & Zenkert, 2009).

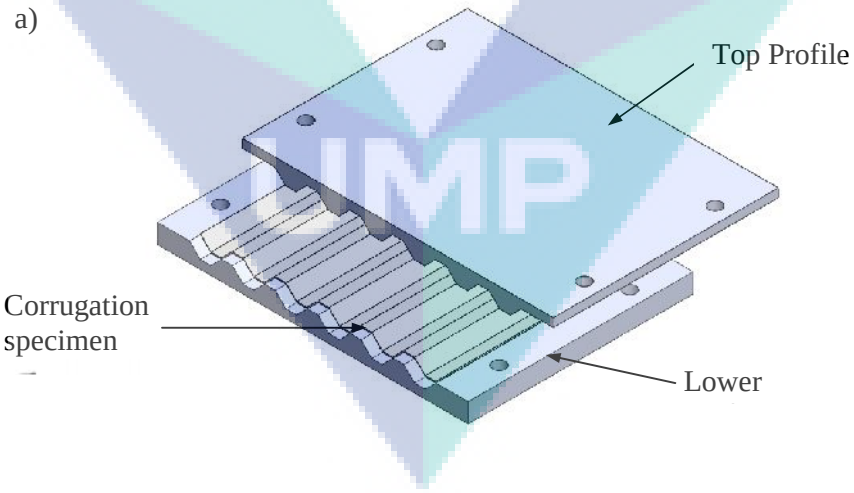

b)

Figure 3.2: a) Solidwork drawing of trapezoidal profile (b) Fabricated mould using CNC machine.

Figure 3.3: Cutting the woven carbon fibre

In order to control the quality of corrugated-core, accurate manufacture procedure is followed. A roll of woven carbon fibre placed on a clean flat surface and was cut according to 210 mm x 230 mm as shown in Figure 3.3. The main advantage of using woven fabric laminates is that it offers properties that are more balanced in the 0° and 90° directions than unidirectional laminates.

Carbon Fibre Reinforced Polymer

Plain weave carbon fibre reinforced polymer (CFRP) was supplied by Easy Composite Ltd, UK (CF-PL-200-100). During manufacturing of the corrugated-core, the mould release gel is applied on the upper and lower moulds. Epoxy mixture resin is then mixed while D.E.R 331 and joint mine 905-3S were used with ratio 2:1. Spread the mixed epoxy resin with the help of brush on the mould. Place the woven carbon fibre fabric on the mould.

Figure 3.4: Layed up process for CFRP

Second layer of mixed epoxy resin is applied on the woven carbon fibre fabric; roller was used with mild pressure on the mat-polymer to remove excess air as shown in Figure 3.4.The process was repeated for each layer until desired ply and thickness achieved. The top mould was placed on the laminate plain weave carbon fibre fabric and then cure for 24 hours at room temperature (T_{room}=28°C).

Glass Fibre Reinforced Polymer

Figure 3.5: Layed up process for GFRP

A woven glass fibre reinforced polymer (GFRP) supplied by Salju Bistari Sdn Bhd, Malaysia was also used in this study. During the manufacturing, the woven glass fibre was cut to dimensions 210 mm x 230 mm and then layer up with mixed epoxy resin as shown in Figure 3.5. The process is repeated for each layer until desired ply and thickness achieved. The top mould was placed on the laminate woven glass fibre fabric and then cure for 24 hours.

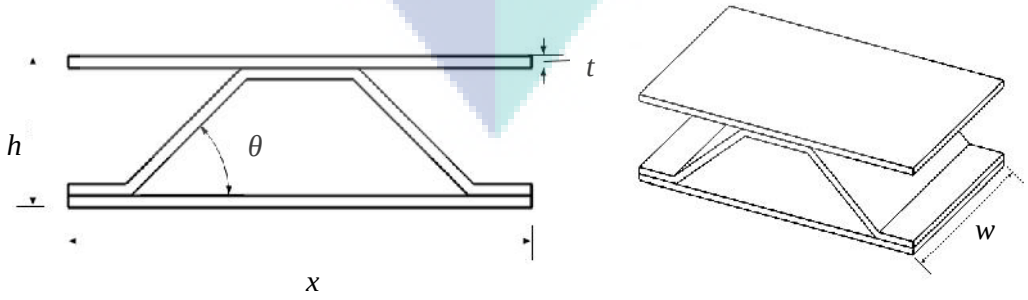

Figure 3.6: The geometry of the trapezoidal corrugated-core sandwich structure

The corrugated-core unit cell is based on trapezoidal profile. The geometry parameters shown in Figure 3.6 are: θ are the internal angle of a unit cell in the trapezoidal corrugated-core sandwich structure; h is the height of the core with skin; t is the average thickness of the wall core and the skin; x is the length of the core and w is the width of the specimen. Due to the mould design, the value of x was 40 mm while θ were set to 45^{o}

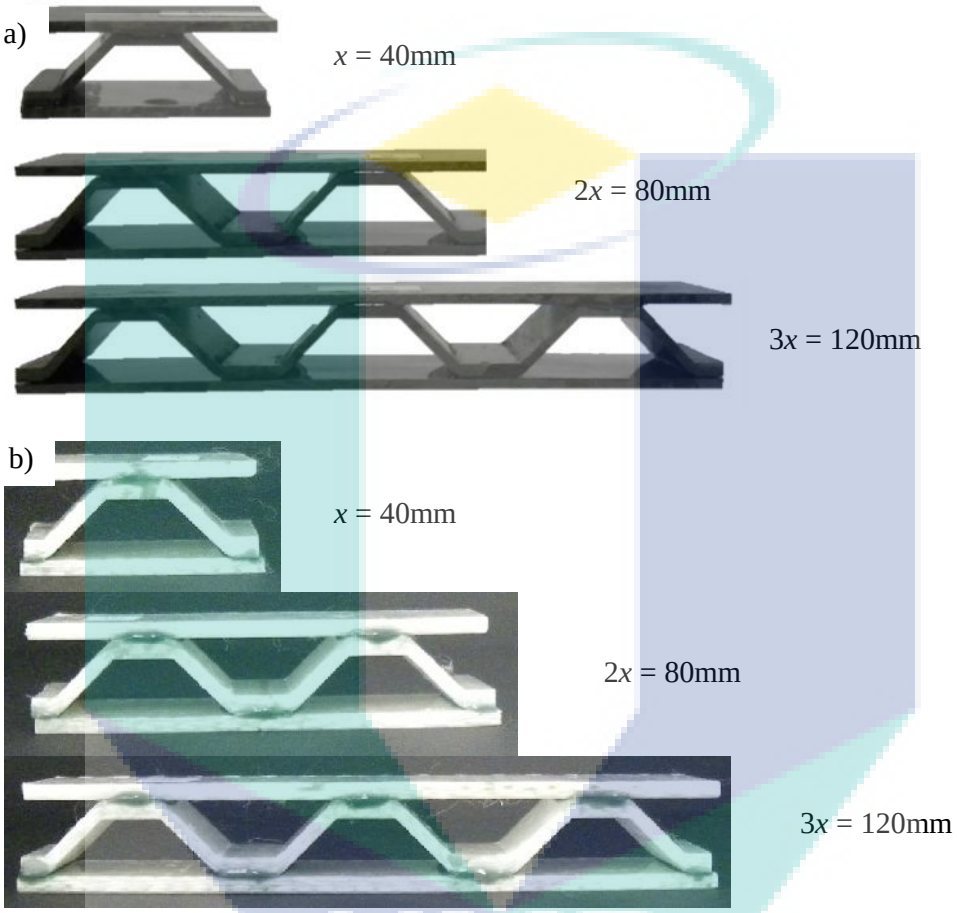

Figure 3.7: a)Photographs of the three different number of unit cell in CFRP and b)Photographs of the three different number of unit cell in GFRP

In preparing the test specimens, the value of w was set equal to 25 mm in width. The corrugated-cores were cut to three different numbers of unit cells as shown in Figure 3.7. The figure shows Carbon Fibre Reinforced Plastic (CFRP) and Glass Fibre Reinforced Plastic (GFRP) with a different number of unit cell.

Mechanical Tests

The mechanical tests were conducted to analyse mechanical properties of the materials.

Tensile Test for CFRP and GFRP plates

Tensile Test on CFRP Plate

Composite layers were fabricated at room temperature in a shape of rectangle plates by hand layup method and appropriate care was taken during fabrication of laminates to ensure equal thickness of materials and to avoid air bubbles. The laminates were fabricated by placing the fibre one over the other with a mixture of epoxy and hardener in between layers. Squeezer was used to distribute resin uniformly, to compact the

plies and removed trapped air or bubble. The surfaces of the laminated were covered with thick plastic to prevent the layup from external disturbances.

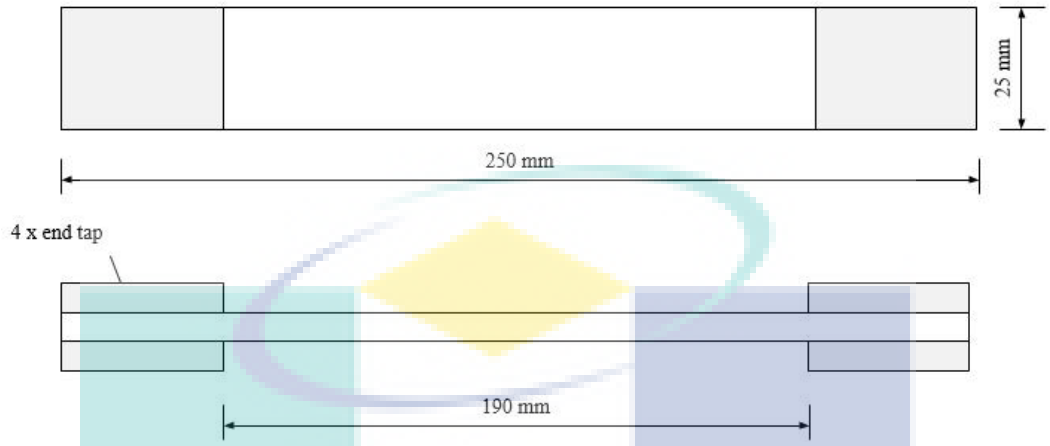

Figure 3.8: Measurement of tensile test specimen

The laminates were cured in room temperature for 24 hours. A jigsaw machine is used to prepare the laminated test specimens to suit ASTM dimension and then the edges were sanded. Figure 3.8 shows drawing of the tensile test specimen, with tab 30 mm.

Figure 3.9: Tensile test setup using Instron machine

Tensile test standard, ASTM D 3039M was used to determine the tensile strength and modulus of the composite. Figure 3.9 shows tensile test setup using Instron machine. Test specimens were sectioned from the composite plates with the width of 25 mm, thickness of 2 mm and length of 220 mm. At least three specimens were prepared using a diamond saw. The specimens were tested using Instron universal test machine at a crosshead speed of 2 mm/min.

The tensile strength (σ) values were calculated by following equation;

$$\pm = \frac{F}{A} \qquad 3.1$$

where F is the ultimate load, and A is the cross-sectional area of the specimen. Elastic modulus was obtained from the initial slope stress (σ) – strain (ε) curves based on the equation below;

$$E = \frac{\pm}{£} \qquad 3.2$$

Table 3.1: Summary of tensile test sample preparation parameter

Type of Fibre	Orientation (°)	*Thickness of ply (mm)	No of ply	Average Total Thickness
CFRP (plain weave)	$[0/90]_8$	0.25	8	2
GFRP (plain weave)	$[0/90]_6$	0.33	6	2

*Thickness according to ASTM D3039

Types of fibre used are plain weave carbon fibre and plain weave glass fibre. The fibre was cut into different size according to ASTM 3039. The orientations of fibre mat are as in Table 3.1.

Static Compression Test

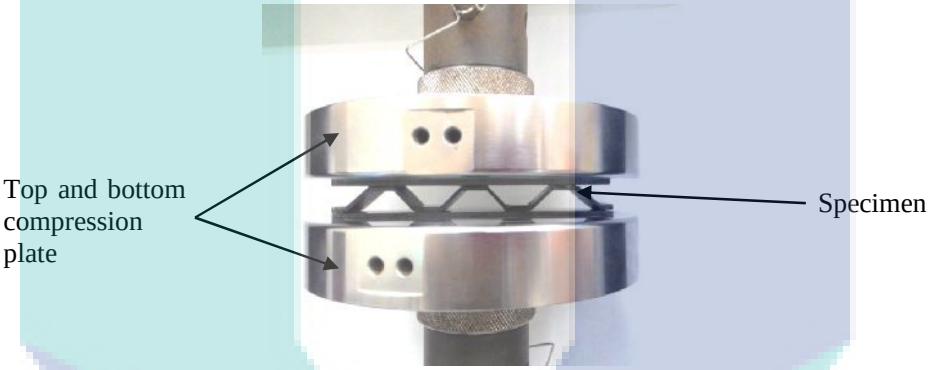

Figure 3.10: Experiment setup for compression test

Compression technique was used to determine compressive stress and compressive strain. Test specimen dimensions are tabulated in Table 3.2. At least three specimens were prepared for every sample. The specimens were tested using Instron Universal test machine at a crosshead speed of 2 mm/min. Figure 3.10 shows experimental setup for compression test.

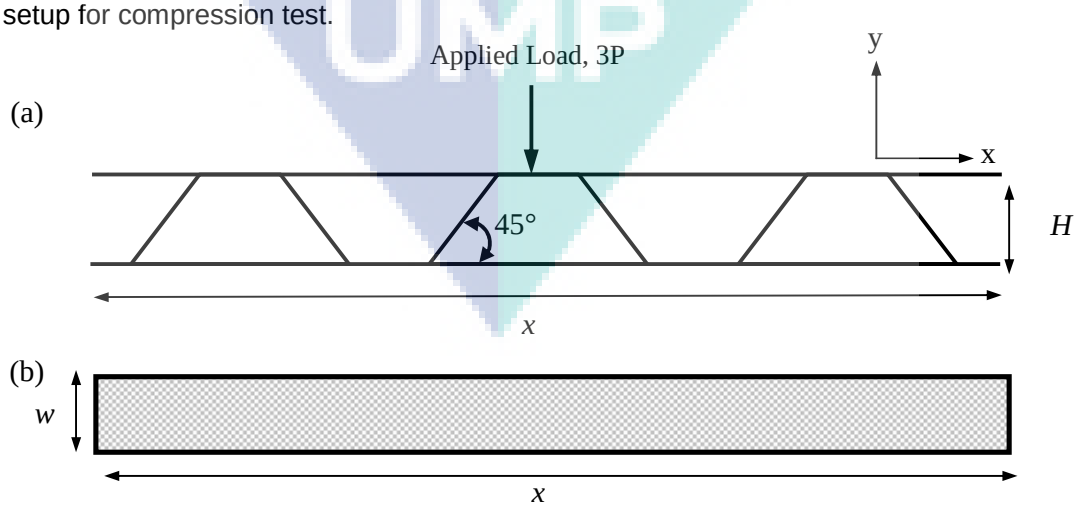

Figure 3.11: (a) Schematic view for compression test (b) Cross-sectional area for compression test

$$Area = w \times x \quad (3.3)$$

Figure Figure 3.11(a) shows schematic view for compression test which the applied load(3P) at 3-unit cell and with angle 45° for every unit cell, *x* and *H* is refer to length and height of the specimen. Figure 3.11(b) shows top surface of the specimen for compression test. Equation 3.3 was used to determine the area of the top surface of the specimen, *w* and *x* refer to width and length of the specimen for compression test. Parameter of CFRP and GFRP corrugated-core sandwich structures are presented in Table 3.2.

Table 3.2: Parameter of composite corrugated-core sandwich structures for compression test

Material	Core ID	No. of unit cell	No. of plies	Average core width, *w* (mm)	Average core length, *x* (mm)	Average core thickness, *H* (mm)
CFRP	**CF1U3P**	**1**	**3**	**25**	**40**	**11.5**
	CF1U4P	**1**	**4**	**25**	**40**	**12**
	CF1U5P	**1**	**5**	**25**	**40**	**12.5**
	CF2U3P	**2**	**3**	**25**	**80**	**11.5**
	CF2U4P	**2**	**4**	**25**	**80**	**12**
	CF2U5P	**2**	**5**	**25**	**80**	**12.5**
	CF3U3P	**3**	**3**	**25**	**120**	**11.5**
	CF3U4P	**3**	**4**	**25**	**120**	**12**
	CF3U5P	**3**	**5**	**25**	**120**	**12.5**
GFRP	**GF1U2P**	**1**	**2**	**25**	**40**	**14**
	GF1U3P	**1**	**3**	**25**	**40**	**16.7**
	GF1U4P	**1**	**4**	**25**	**40**	**18.5**
	GF2U2P	**2**	**2**	**25**	**80**	**14**
	GF2U3P	**2**	**3**	**25**	**80**	**16.7**
	GF2U4P	**2**	**4**	**25**	**80**	**18.7**
	GF3U2P	**3**	**2**	**25**	**120**	**14**
	GF3U3P	**3**	**3**	**25**	**120**	**17**
	GF3U4P	**3**	**4**	**25**	**120**	**18.7**

Analytical Model of Compression Response of Corrugated-core Sandwich Structure

Consider trapezoidal corrugated-core model with geometrical quantities as stated in Figure 3.12(a) which is exposed to an applied load. When the sandwich structure is subjected to a compressive load 3P, it is assumed that all of the unit cells are applied to the same load, as shown in Figure 3.12(b). Each of the core unit cells can be considered as a cantilever beam subjected to the same axial compression load *N*, bending moment *M* and shear load *R*, as showed in Figure 3.12(c). Here, no deformation is allowed at the end of the lower unit cell.

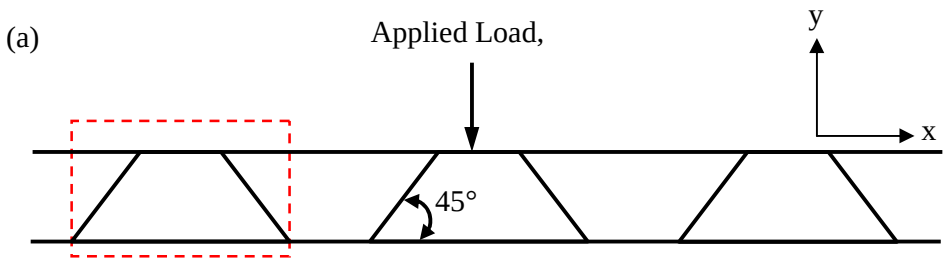

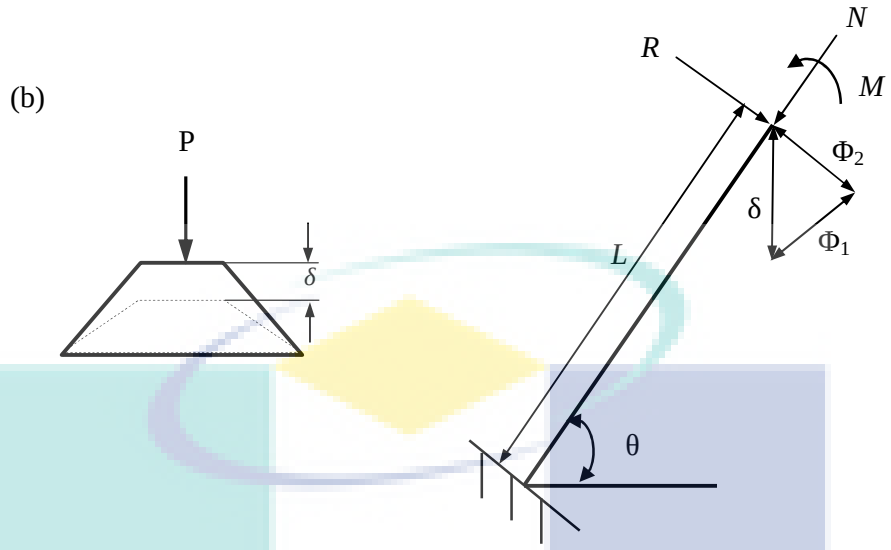

Figure 3.12: (a) A three unit cell sample under compression loading, (b) a single unit cell shows the deformed behaviour (dashed-line), (c) a free-body diagram of a compression loaded core member

Considering equilibrium of loads in y-direction, it can be shown that:

$$N \sin \theta + R \cos \theta = \frac{P}{2} \qquad 3.4$$

and the bending moment M and the shear load R are related through:

$$M = \frac{RL}{2} \qquad 3.5$$

The deformation δ then can be written in terms of the displacement parameters of Φ_1 and Φ_2 as:

$$\Phi_1 \sin \theta + \Phi_2 \cos \theta = \delta \qquad 3.6$$

where the relationship between the Φ_1 and Φ_2 is:

$$\Phi_1 = \Phi_2 \tan \theta \qquad 3.7$$

and based on classical beam theory, the relationship between the displacement parameters and the loads acting on the core member can be written as follows:

$$\Phi_1 = \frac{NL}{EA} \quad ; \quad \Phi_2 = \frac{RL}{12EI} \qquad 3.8$$

where A is the cross-sectional area (= wH), I is the second moment of area (=wH^3/12) and E is the Young's modulus of the core. Substituting Equations 4 and 5 into Equation 3, and then solving using Equation 1, the relationship between the load P and the deformation δ can be shown to be:

$$P = \frac{2EHw\,(L^2 \sin^2 \theta + H^2 \cos^2 \theta)}{L^3} \delta \qquad 3.9$$

In predicting the strength of the model, Euler buckling and core shear buckling are two possible modes of local elastic buckling in the inclined cell wall under lateral

compression load. Here, the Euler buckling load P_E, can be estimated from classical buckling theory as:

$$P_E = \frac{\pi^2 EI}{L^2} \qquad 3.10$$

where λ is a factor dependant on the boundary conditions. Assuming perfect bonding between the core and the skins, the value of P_E for a corrugated structure here can be expressed as:

$$P_E = \frac{n\pi^2 EwH^3\left(L^2 \sin^2\theta + H^2 \cos^2\theta\right)}{6L^4 \sin\theta} \qquad 3.11$$

Since $\theta = 45^o$ in this study, Equation (8) can be simplified as:

$$P_E = \frac{nEwH^3}{6\sqrt{2}}\left(\frac{\pi}{L}\right)^2\left\{1+\left(\frac{H}{L}\right)^2\right\} \qquad 3.12$$

Static Tensile Test for corrugated-core

Tensile technique was used to determine tensile stress and strain. Test specimen dimension as shown in Table 3.3. At least three specimens were prepared for every sample. Instron Universal test machine at a cross section speed 2 mm/min is used to test the specimens. The average tab length is 8 to 9 mm. Equation 3.13 is used to determine the cross-sectional area for the trapezoidal corrugated-core.

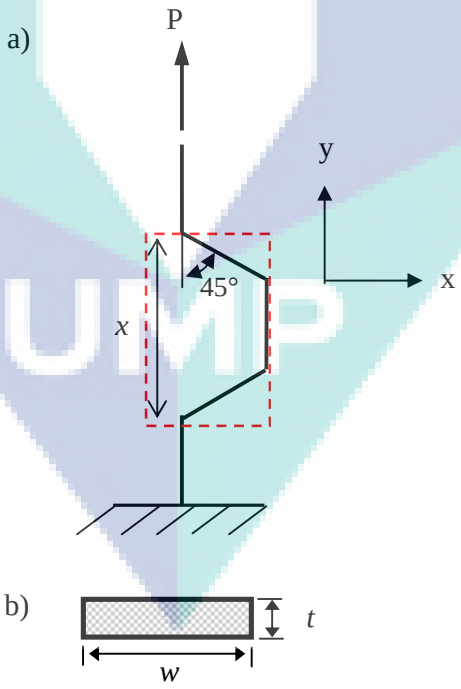

Figure 3.13: (a) Schematic view for tensile test (b) Cross sectional area for tensile test of trapezoidal corrugated-core

Figure Figure 3.13(a) shows schematic view for tensile test which show the gauge length, *x* and the corrugation angle 45°. Figure 3.13(b) shows cross sectional area for corrugated-core tensile test.

$$Area = w \times t \qquad 3.13$$

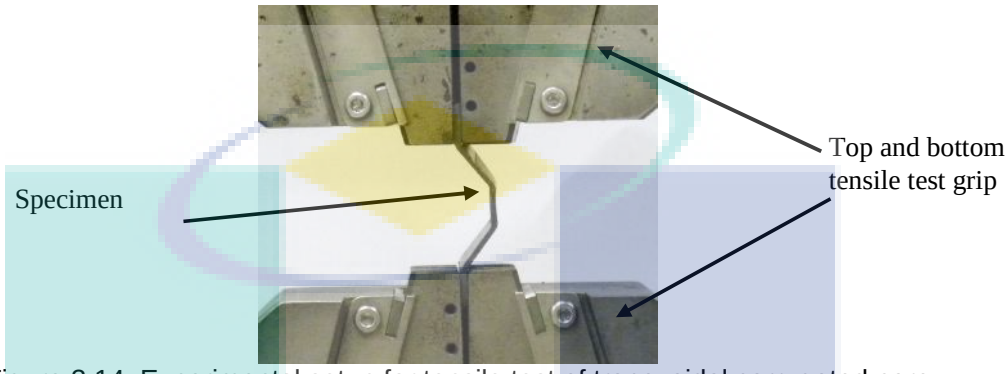

Figure 3.14: Experimental setup for tensile test of trapezoidal corrugated-core

Figure 3.14 shows experimental setup for tensile test of trapezoidal corrugated-core which shows the one-unit cell specimen and the top and bottom of the tensile test grip/clamp. Table shows parameter for tensile test trapezoidal corrugated-core.

Table 3.3: Parameter for tensile test trapezoidal corrugated-core

Material	Core ID	No. of unit cell	No. of plies	Average core width, *w* (mm)	Average gauge length, *x* (mm)	Average laminate thickness, (mm)
CFRP	**CF1U3P**	**1**	**3**	**25**	**30**	**1.75**
	CF1U4P	**1**	**4**	**25**	**30**	**1.85**
	CF1U5P	**1**	**5**	**25**	**30**	**1.95**
	CF2U3P	**2**	**3**	**25**	**70**	**1.75**
	CF2U4P	**2**	**4**	**25**	**70**	**1.85**
	CF2U5P	**2**	**5**	**25**	**70**	**1.95**
	CF3U3P	**3**	**3**	**25**	**110**	**1.75**
	CF3U4P	**3**	**4**	**25**	**110**	**1.85**
	CF3U5P	**3**	**5**	**25**	**110**	**1.95**
GFRP	**GF1U2P**	**1**	**2**	**25**	**30**	**1.85**
	GF1U3P	**1**	**3**	**25**	**30**	**2.60**
	GF1U4P	**1**	**4**	**25**	**30**	**3.5**
	GF2U2P	**2**	**2**	**25**	**70**	**1.85**
	GF2U3P	**2**	**3**	**25**	**70**	**2.60**
	GF2U4P	**2**	**4**	**25**	**70**	**3.5**
	GF3U2P	**3**	**2**	**25**	**110**	**1.85**
	GF3U3P	**3**	**3**	**25**	**110**	**2.60**
	GF3U4P	**3**	**4**	**25**	**110**	**3.5**

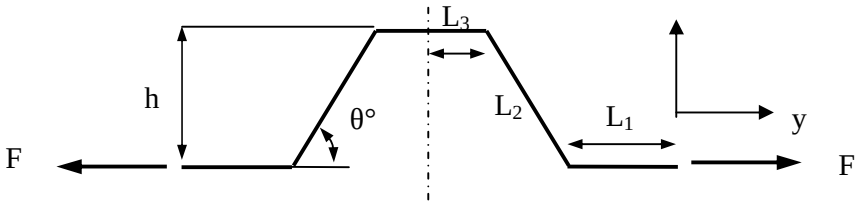

Figure3.15: Schematic diagram of corrugated-core for tensile loading

To calculate the tensile displacement of corrugated-core, a unit cell of corrugated-core was considered as shown in Figure 3.15. Since the unit cell is symmetric along the axis passing through the middle of the unit cell, half of the unit cell was used in calculation. The strain energy of each member is due to bending and axial forces (Dayyani et al., 2011),

$$Ui = Ui, tension + Ui, bending, i = 1,2,3 \qquad 3.14$$

Finally, the force-displacement relation is:

$$F = 196.2 \qquad 3.15$$

In which the units of displacement and force are (mm) and (N), correspondingly. The strain energy of each member is due to bending and axial forces as mentioned in Thill et al., 2010.

$$Ui = \int_0^{li} \frac{Fi^2}{2EA} dx_i + \int_0^{li} \frac{Mi^2}{2EI} dx_i \qquad 3.16$$

Where in deformed shape bending moment and axial forces are:

$$Mi = Fh/2, Fi = F, i = 1,3 \qquad 3.17$$

$$Mi = \left(F \sin^{-}\right)^{*} xi - \left(F \sin^{-}\right) l_2 / 2, Fi = F \cos^{-}, i = 2 \qquad 3.18$$

By substituting the dimension of unit cell from figure, the strain energy of the members would be calculated as:

$$U_1 = \int_0^{10} \frac{F^2}{2EA} dx + \int_0^{10} \frac{5F^2}{2EI} dx \qquad 3.19$$

$$U_2 = \int_0^{\sqrt{200}} \frac{\left(\left(F \sin^{-}\right) * x_i - \left(F \sin^{-}\right) l_2 / 2\right)^2}{2EA} dx + \int_0^{\sqrt{200}} \frac{\left(F \cos^{-}\right)^2}{2EI} dx \qquad 3.20$$

$$U_3 = \int_0^{10} \frac{F^2}{2EA} dx + \int_0^{10} \frac{5F^2}{2EI} dx \qquad 3.21$$

The total strain energy is:

$$U = U_1 + U_2 + U_3 \qquad 3.22$$

Using Castigliano's theorem, the total tensile displacement of half of single trapezoidal corrugated unit cell, δ, is then:

$$¢ = \frac{\partial U}{\partial F} = 4F\left(\frac{10}{2EA} + \frac{125}{2EI} + \frac{100\sqrt{200}}{24EI} + \frac{25}{2\sqrt{200}EA}\right) \quad 3.23$$

Finite** **Element Analysis

In modelling and simulation of the corrugated-core are done by Finite Element (FE) software to model the response of the specimens under static and dynamic loading. The simulation is to compared to the experimental results in order to validate the numerical models using Finite Element Analysis (FEA). ABAQUS/CAE version 6.13 was used for modelling, submitting, monitoring and visualising the results. Thus, after the parameter and boundary condition used as input in this simulation, failure criteria can be predicted according to the load applied and shape of the corrugated-core. The expected result is to get the failure criteria through the corrugated structure with variation in time domain.

ABAQUS is a group of powerful engineering simulation programs, based on the finite element method that can solve problems from relatively simple linear analyses to the most challenging nonlinear simulations (Simulia, 2012). ABAQUS has an extensive library of elements that can model virtually any geometry. It has an equally wide list of material models that can simulate the behaviour of most typical engineering materials including metals, rubber, polymers, composites, reinforced concrete, crushable and resilient foams, and geotechnical materials such as soils and rock. Designed as a general-purpose simulation tool, ABAQUS can be used to study more than just structural (stress/displacement) problems. It can simulate problems in such diverse areas as heat transfer, mass diffusion, thermal management of electrical components (coupled thermal-electrical analyses), acoustics, soil mechanics (coupled pore fluid-stress analyses), piezoelectric analysis, and fluid dynamics. ABAQUS offers a wide range of capabilities for simulation of linear and nonlinear applications. Problems with multiple components are modelled by associating the geometry defining each component with the appropriate material models and specifying component interactions. In a nonlinear analysis, ABAQUS automatically chooses appropriate load increments and convergence tolerances and continually adjusts them during the analysis to ensure that an accurate solution is obtained efficiently.

Modelling

In modelling part, the dimension of the corrugated-core has been calculated and drawn inside ABAQUS software using ABAQUS/Standard. 3D modelling was chosen, the type of the part is deformable and shell extrusion.

Pre-setup for corrugated-core structure

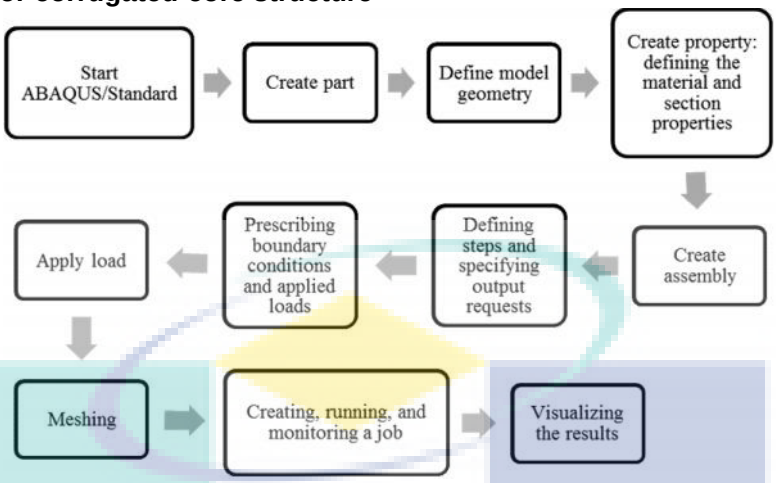

Figure 3.16: The flow process to set up in ABAQUS

Figure 3.16 shows the flow process to be set up in ABAQUS software. Simple and easy explanation of the set up as follows. In create part; choose 3D as the modelling space, type deformation and the base feature shape and type is shell and extrusion. After that, create property which defining the material and section properties. In material, select elastic properties with isotropic type. Next, section shell and homogeneous were selected thus create the assembly. Then, define the steps and specify output requests with initial = 0.005, minimum = 0.000001 and maximum = 1. Create field output, choose whole model and select from list. Create history output, Domain set platen and select from the list for displacement and force/reaction. Create interaction surface to surface contact for upper platen, corrugated and lower platen. In load toolbox, create boundary condition for top and bottom of the platen and mesh the assembly. Create and submit job and monitor the job and lastly visualise the complete result.

Modelling of Compression Trapezoidal Corrugated-core Sandwich Structure

In this section, the Finite Element Modelling procedures are shown to develop simulation. In order to create a new model inside ABAQUS, there are few steps to be carried one by one until it is finished. For the trapezoidal corrugated-core, the first step is to create the part. This is done by clicking on Part Icon on toolbox area at the left side of the viewport. The reason behind this is to build the trapezoidal corrugated-core in the shape and dimension as desired.

Upon creating a new part, use modelling space 3D with deformable type. For the based feature, shell shape is used since the trapezoidal has thin thickness. Type extrusion is used to extrude the part. An interface will be shown in order to give a workspace to create a new part by drawing it. Since the trapezoidal corrugated-core is quite simple in its shape, the drawing process is quite simple. Set the workspace in order to create a 3D object, the software will generate a viewport with 2D grid, with several drawing icons on the left side of the workplace. To create the trapezoidal corrugated-core, draw as 2D drawing.

After the drawing is completed, the software will ask the desired depth for 3D object to create, set it to be 25 mm similar as specimen's width. Since the model is in millimetre, the depth of the model should be written as 25. A trapezoidal shape part will be automatically drawn in 3D to be ready to use later, as can be seen here in Figure 3.17.

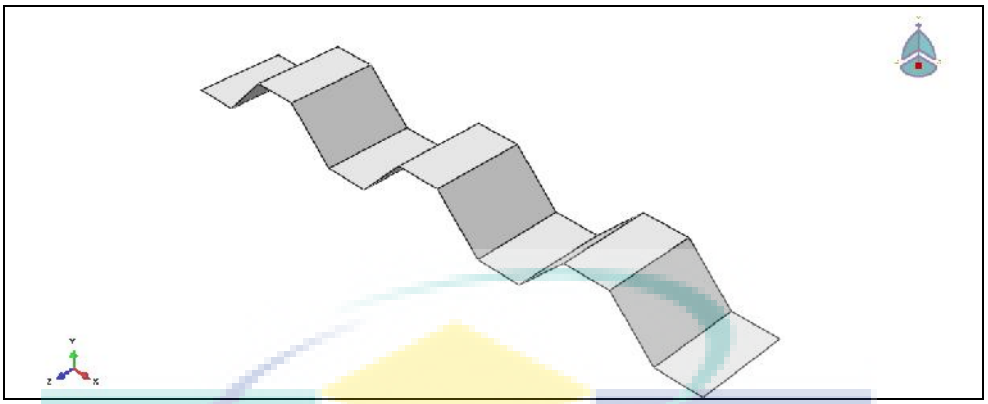

Figure 3.17: Completed part of Trapezoidal Corrugated-core

After completing the component parts of the trapezoidal, continue to set the properties in the modelling. As mentioned, use CFRP and GFRP for the structure of buckling trapezoidal corrugated-core due to its high strength to weight ratio, to analysed buckling phenomena. In order to insert material in ABAQUS, click on create Materials icon at Toolbox area. In this case, by rename the material as CFRP and set the basic properties of CFRP, for example the elasticity property would be important. In buckling trapezoidal corrugated-core model, elastic property would be a good choice for the model. Subsequently, by setting materials Poisson's Ratio and Young's Modulus, get the desired mechanical properties of the CFRP-made buckling trapezoidal corrugated-core. This time, Young's Modulus of CFRP is based on experimental data to validate between FEM analysis and experimental. Add stress property for CFRP properties with yield stress of 503.85 MPa. Table shows input data for finite element modelling; the input data is obtained from experimental analysis.

Table 3.4: Input data for finite element modeling

Properties	Value
Young Modulus (E_{11} & E_{22})	**21236 N/mm^2**
Ultimate Strength (X^T)	**503.85 MPa**
Poison's Ratio	**0.1**

The following step in the model would be defining the section property of the trapezoidal corrugated-core. By creating a new section property, define the trapezoidal corrugated-core as a shell of section. Then, by clicking on Section Icon in Toolbox area, choose shell homogenous property since the trapezoidal corrugated-core should have a thin section, not solid or others. In the section setting, connect the materials property that have been created earlier with the part that we want to fabricate with the material.

Once succeed with producing the section property, set the section assignments for the whole trapezoidal corrugated-core itself. This is done by clicking the part module at Model tree, choose the trapezoidal corrugated-core model at the viewport. This action will cause the border of the trapezoidal corrugated-core to be red in colour, and a window named Edit Section Assignment will pop out. Choose shell offset as the middle surface. Click OK to accept the setting.

The following step in this task would be setting the assembly for the trapezoidal corrugated-core. This step is important as this is to specify how this model is assembled; if there are some parts created in the model; how these parts are positioned and oriented in the simulation. These are done by clicking the instance icon,

placed right under the assembly icon in Toolbars, and then, just choose the upper platen, lower platen and the trapezoidal available in the list, and click OK. Organise the part using translate instance. The example of the task is shown here, in Figure 3.18.

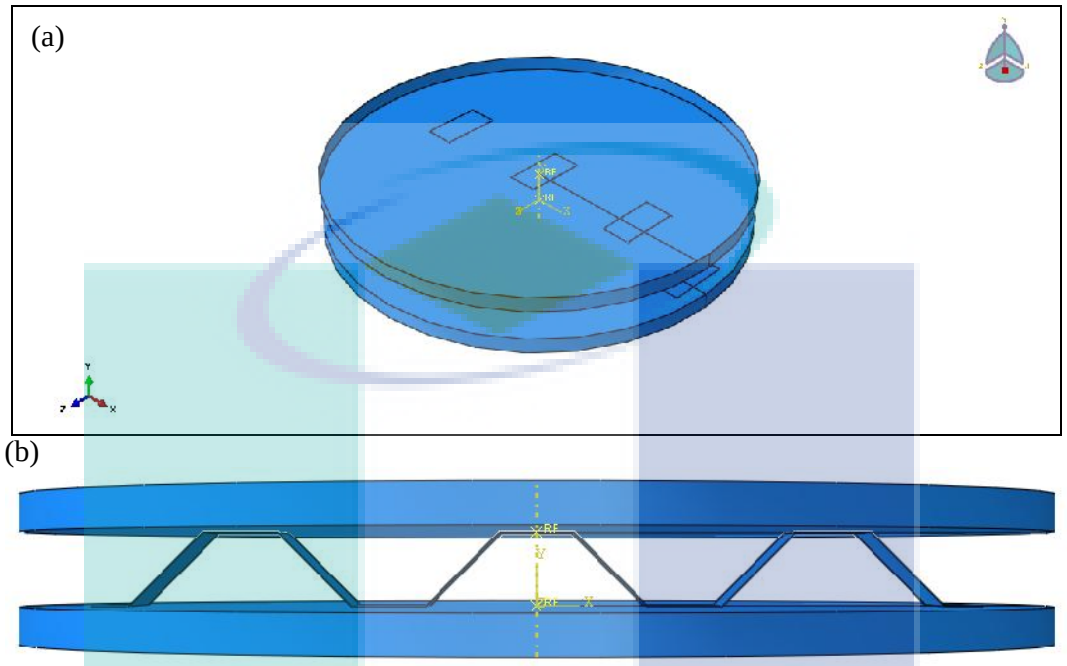

Figure 3.18: Arranging the instance for the model, (a) Isometric view, assembly of a sandwich structure between two platens, (b) Front view of the model

After the arrangement of the instance, proceed by creating a new Step property. In ABAQUS, the step is like a framework in which to set sequential timeline during the simulation. To put it simple, it is like how to set the initial behaviour of the model (before simulation) and what would happen when simulation starts. In this case, since it has set the timeline like, before the simulation starts, no load and movement occurs, then, the simulation will start right when applying load, platen and the structure movement. Therefore, it is obvious that it should have an initial step for setting before loading applied, and another step after that, when starting the simulation, and loading takes place on the model.

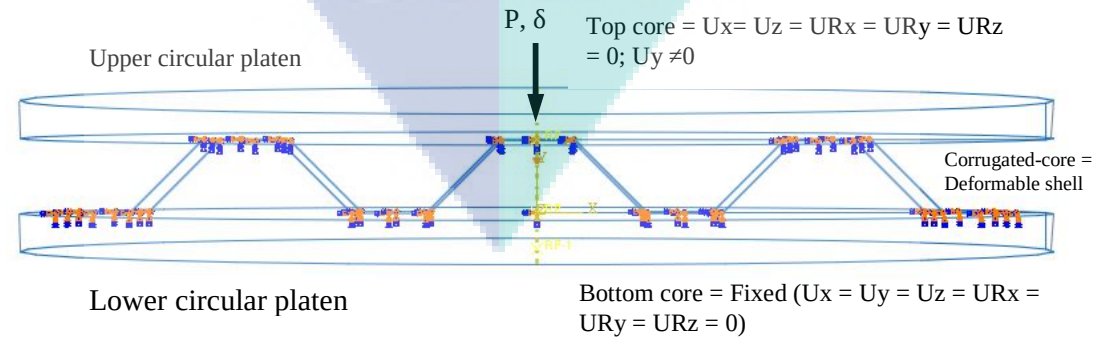

Figure 3.19: Setting for boundary condition

When creating the boundary conditions, the nodes along the top and bottom edges were fully constrained, except in y-direction (Uy ≠ 0) at the upper edge as shown in Figure 3.19. This is to allow the upper edge to move downwards. A displacement

boundary condition was applied uniformly to the nodes at the top of the unit cells to progressively crush the unit cells. This displacement boundary condition was assigned to the reference point, placed at the centre of the upper platen, and this was set to displace the platen downwards in vertical direction at a constant rate. The reference point was used to record the displacement and reaction load from the core.

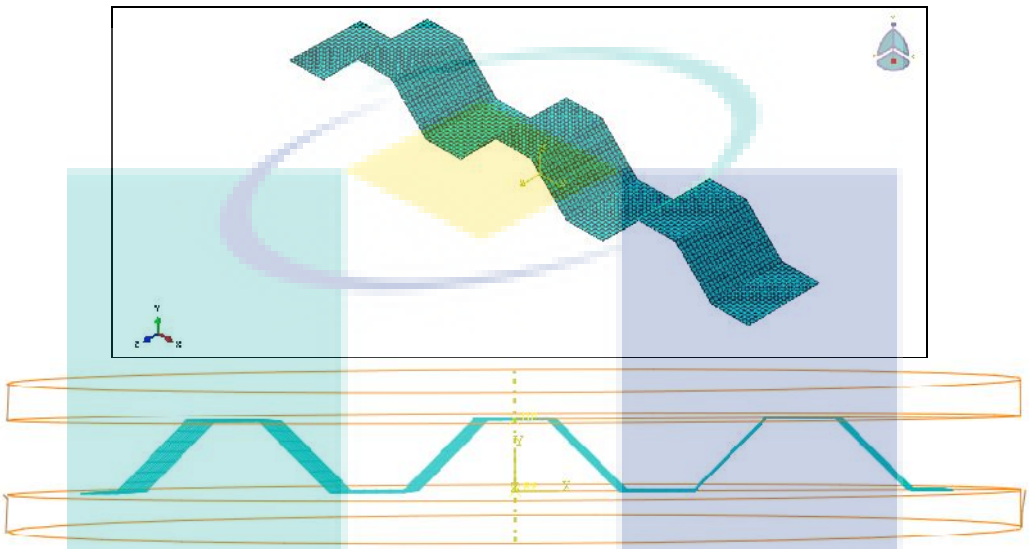

Figure 3.20: Configuring for meshing

A mesh was then generated at a corrugated-core based on three unit cells using the meshing tools in ABAQUS/CAE. Figure 3.20 shows the model used in the compression simulation study, comprising 25 linear shell elements across the width direction and 14 elements along the length of the struts, giving a total of 3500 elements. For the platen, there is no mesh required for an analytically rigid surface. The default form of hourglass control available for the S4R element was used as well as reduced integration. Hourglass control attempts to minimise spurious modes without introducing excessive constraints on the physical response of the element.

Model Sensitivity

The exactness of the model can be improved in many ways. Imperfections from uneven cell wall thickness, sensitivities of the mesh refinement, the contact stiffness between the platen and the core can cause inaccuracy towards the analysis. Finally, the selection of the suitable type of shell element for the model is clearly essential.

Contact Stiffness

In the actual specimen preparation, the corrugated-core was bonded to the skins, and therefore there is a softening associated with the epoxy adhesive. Figure 3.21 shows hard contact data form FEM before including the contact stiffness. To account for such effects, a linear softened contact pressure-over closure formulation was employed during the initial stage of contact between the sharp edge of the core and the platen. The softened contact pressure-over closure relationships might be used when modelling a soft, thin layer on one or both surfaces. It should be noted that for the initial numerical predictions, based on FE-Perfect model, the predicted peak load and stiffness are higher for all types of composites corrugation. From the imperfection-sensitivity procedure and the analysis data, an initial imperfection with amplitude of 0.03 was introduced into both the GFRP and CFRP models with contact stiffness 100.

Following this, the comparison between the numerical and experimental results was reasonably good. Figure 3.22 shows contact stiffness comparison.

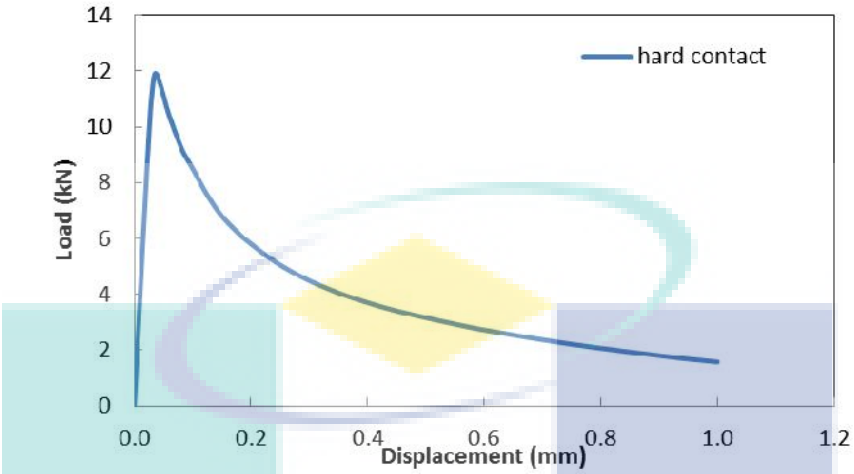

Figure 3.21: Hard contact data from FEM

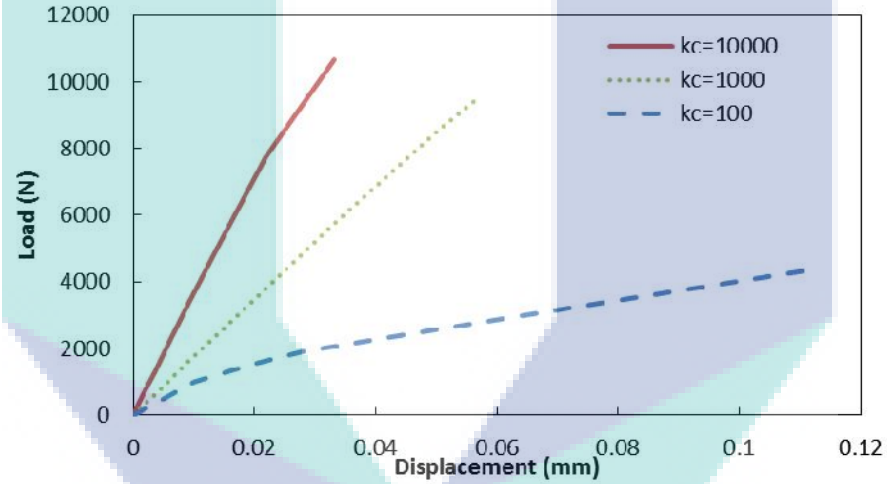

Figure 3.22: Contact stiffness comparison, from kc = 100 to 10000

Modelling of Tensile Corrugated-core Sandwich Structure

Modelling of tensile corrugated-core sandwich structure is similar to the modelling of compression analysis. Only that the model of the part specimen, load and the step were changed. Boundary condition applied shown in Figure 3.23 which includes fixed end and load. Figure 3.24 shows meshing for tensile analysis, it has 1092 nodes, 1001 element and the element type is S4R. The element type is quadrilateral. The simulation was then submitted for job analysis and the data were analysed.

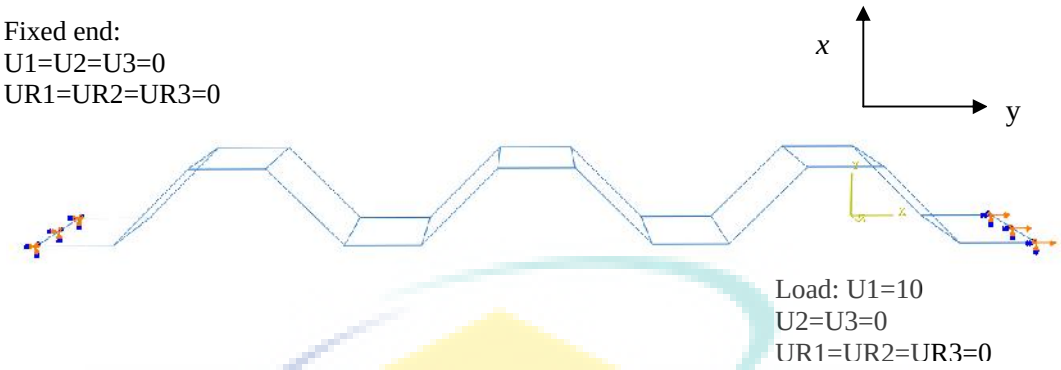

Figure 3.23: Boundary condition applied in modelling of tensile analysis

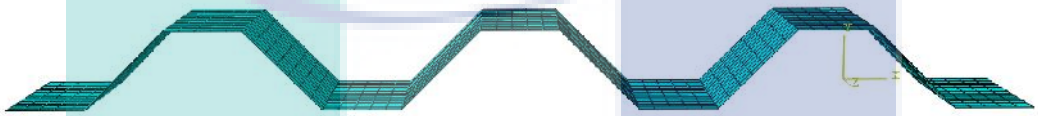

Figure 3.24: Meshing for tensile test analysis

4. FINDINGS

In this section, the experimental results and finite element modelling obtained during this research are presented. The results from tensile test and compression test will be studied and analysed. Furthermore, the behaviour of the structures under compression loading will be discussed.

Mechanical Properties of Materials

This section discusses the results obtained from a series of tensile test on the CFRP and GFRP laminates. One of many ways to find out mechanical properties of materials is by using the tensile test. The tensile test itself is used to find out and evaluate the strength of material that being tested. By delineation, tensile test is the measurement of the ability of a material to withstand the forces of pulling the sample apart and extend it before it breaks.

Tensile Test on Carbon Fibre Reinforced Plastic (CFRP) and Glass Fibre Reinforced Plastic (GFRP)

To identify the required mechanical properties of the laminates used in dealing with of sandwich material, the tensile tests were executed. Tensile tests are conducted on the CFRP and GFRP composite laminates using Instron Universal Testing Machine at crosshead speed of 2mm/minute. Three specimens of the composite sample were experimented corresponding to ASTM D3039 standard as a basic for tensile standard testing (Dayyani et al., 2012).

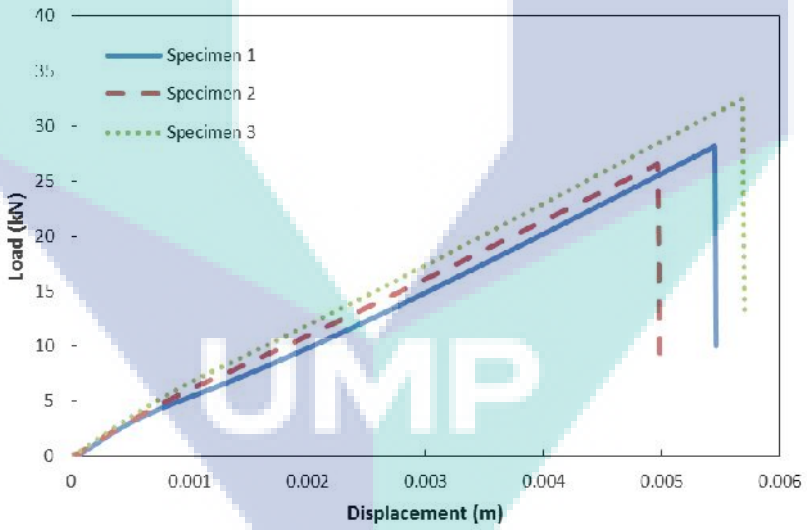

Figure 4.1: Tensile Load-Displacement Curve for CFRP specimens

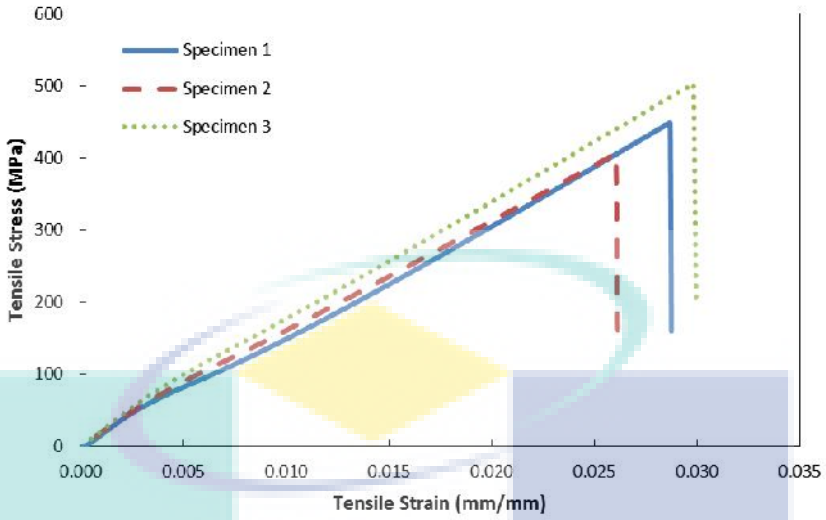

Figure 4.2: Tensile Stress-Strain Curve for CFRP specimens

After going through experiment process, Figure 4.1 and Figure 4.2 show the load-displacement curve and stress-strain curve. The composite laminate exhibited a rough linear response up to the maximum stress value. At this point, the composite failed causing sudden great damage across the width of the sample and exhibited brittle behaviour, as shown in Figure 4.3. When brittle material is subjected to load, it will fail (break) with little deformation. The yield point, and the failure point are similar for brittle material. The maximum load is 32.42 kN, showed in Figure 4.1. Stress-strain curve for CFRP specimens are shown in Figure 4.2. The ultimate tensile stress is at 503.85 MPa respectively.

(a)

(b)

(c)

Figure 4.3: Tensile test after testing: a) Specimen 1, b) Specimen 2, c) Specimen 3

During the test, cracking sound detected due to fibre breaking and delamination. A sudden exploding sound spotted when the specimen break at ultimate (Figure 4.2). Tensile failure code in Figure 4.3 shows at specimen 1, it breaks near at the top tab which is Lateral At tab Top (LAT), specimen 2 break in the tab, Lateral Inside tab Top (LIT) and specimen 3 breaks near at top and bottom of the tabs. All three specimens have different failure code/typical modes, this may be due to laminating problem, gripping and different thickness. Failure code/typical mode is to record the mode and location of failure of the specimen according to standard description using the three-parts failure mode code.

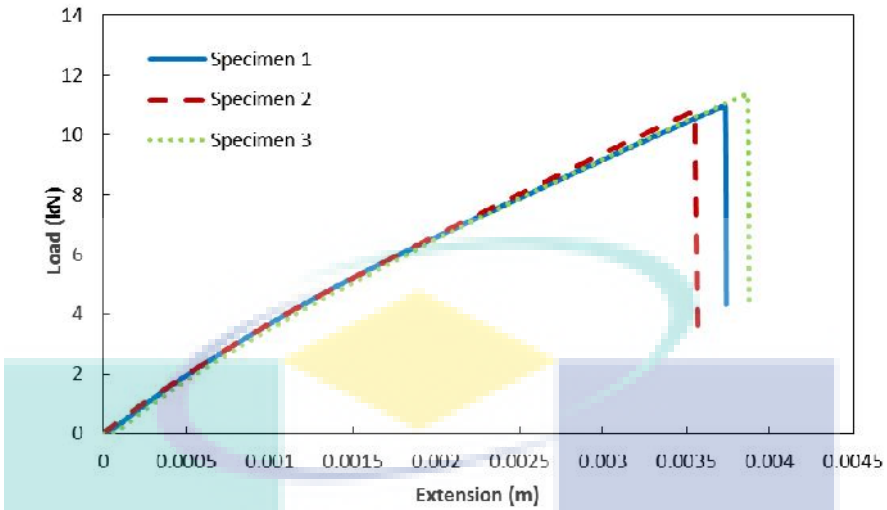

Figure 4.4: Tensile Load-Displacement Curve for GFRP specimens

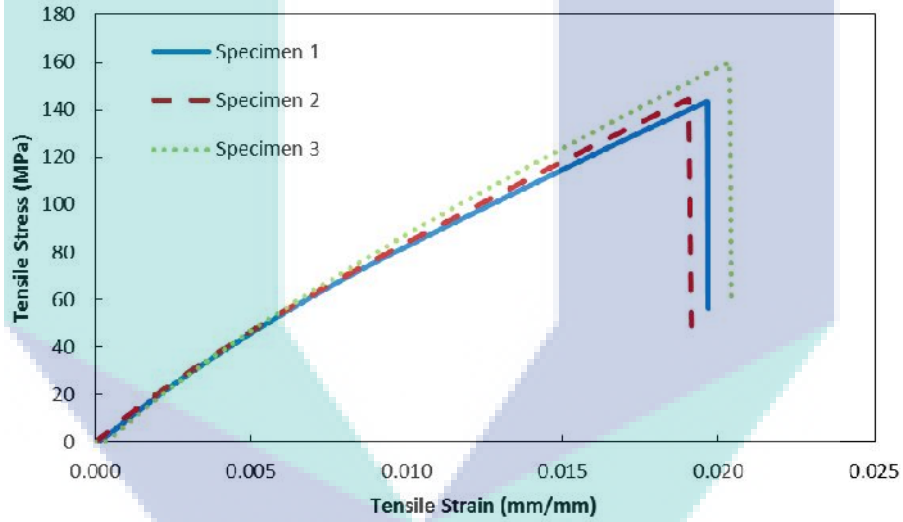

Figure 4.5: Tensile Stress-Strain Curve for GFRP specimens

Figure 4.4 shows a load-displacement curve with the highest load 11.36 kN and Figure 4.5 shows stress-strain curve with ultimate tensile stress at 161.17 MPa. Same as the CFRP specimens in tensile test, the composite laminate exhibited a rough linear response up to the maximum stress value. Here, the composite failed causing sudden great damage across the width of the sample, as shown in Figure 4.6. Specimens for both CFRP and GFRP failed in brittle behaviour which is typical failure for polymer matrix composite. Tensile stress for CFRP specimen is higher than GFRP specimen as shown in the graph. CFRP specimen has a higher elastic modulus and lower density than GFRP specimen, with a combination of lightweight, very high strength and high stiffness (Smith & Hashemi, 2001). These properties make the use of CFRP attractive for aerospace application.

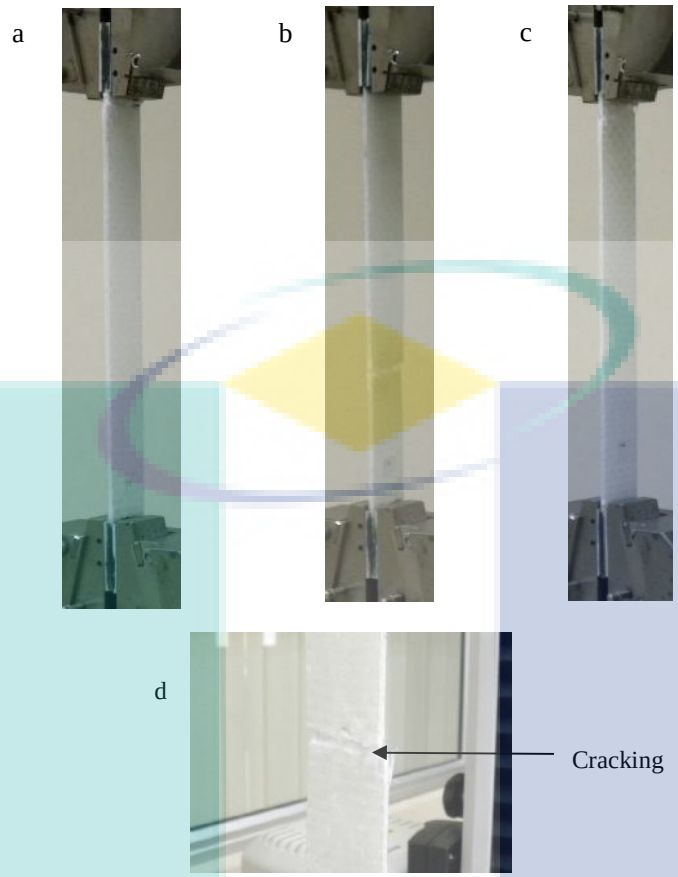

Figure 4.6: Tensile test GFRP after testing: a) Specimen 1, b) Specimen 2, c) Specimen 3, d) Example of cracking

Tensile failure mode for GFRP in Figure 4.6 shows at specimen 1, it breaks near the top tab which is Lateral At tab Top (LAT), specimen 2 break in the middle, Lateral Gage Middle (LGM) and specimen 3 breaks near at top tab, Lateral At tab Top (LAT). Here, the composite laminates display a rough linear response up to the maximum stress value. At this point, the composite failed in a devastating manner across the width of the sample, as shown in Figure 4.6(d), cause abrupt rupture and rapid drop in the stress-strain curve. The specimens have different failure mechanism, this may be due to gripping, laminating problem and different thickness.

Static Compression Test for Sandwich Corrugated-core Structure

Compression tests were carried out to determine the compression strength and stiffness of the specimens under compression loading.

The Compression Behaviour of CFRP Trapezoidal Corrugated-core Sandwich Structure

Compression tests on the corrugated-core sandwich structure were conducted using Instron series testing machine with a crosshead speed of 2mm/min. CFRP trapezoidal corrugated-core sandwich structure shows brittle behaviour of material crushing under compression load as shown in Figure 4.7.

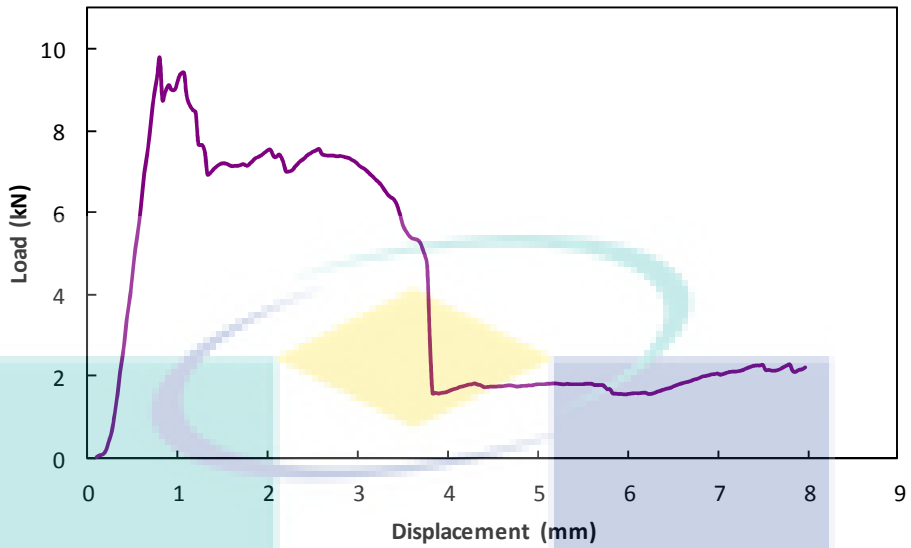

Figure 4.7: Graph of Load-Displacement Curve for 3U5P (three unit cells and five plies) CFRP Corrugated-core Sandwich Structure

Figure 4.7 shows example graph of load-displacement curve of three-unit cells corrugated core sandwich structure with five plies. Upon loading, the specimen shows nonlinear response during the early loading stage. This maybe attributes to the machine compliance and perhaps more significantly, to the fact that closer inspection revealed that both skins were not parallel to each other.

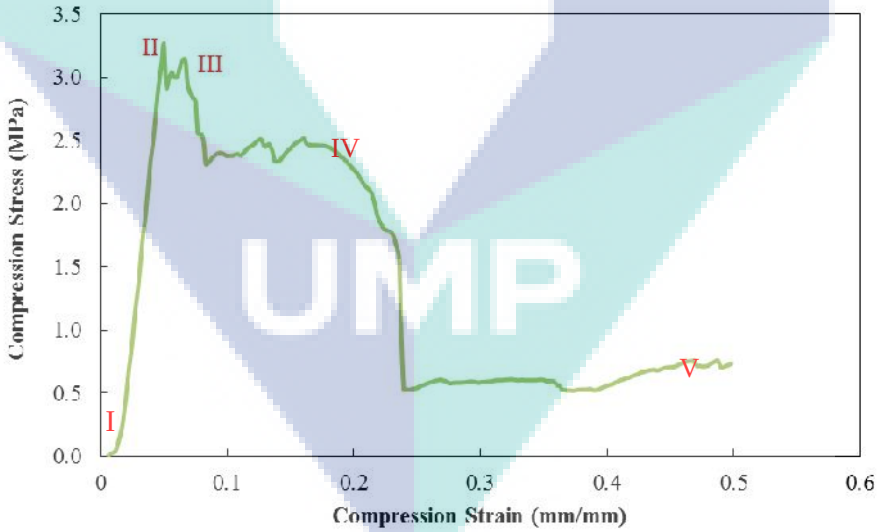

Figure 4.8: Graph of Stress-Strain Curve for 3U5P CFRP Corrugated-core Sandwich Structure

The failure processes in CFRP trapezoidal corrugated-core are shown in Figure 4.8 and Figure 4.9(a) shows the deformation behaviour of compression CFRP corrugated-core structure. The initial failure starts with debonding at the end of right and left specimen followed by sudden break at II which cause the compression stress to decrease and increase again at III as the structure still have two more unit of cells that still in good condition. In Figure 4.8, I indicates elastic region which if load release at

this region, the specimen will get back to original dimension. The strut starts to fracture at IV in all unit cells and decrease drastically. Following failure include delamination, fibre breaking and debonding (III-VI). The figure shows brittle materials break at the stress maximum and at low strain. This condition also observed by (Rejab et al., 2016)

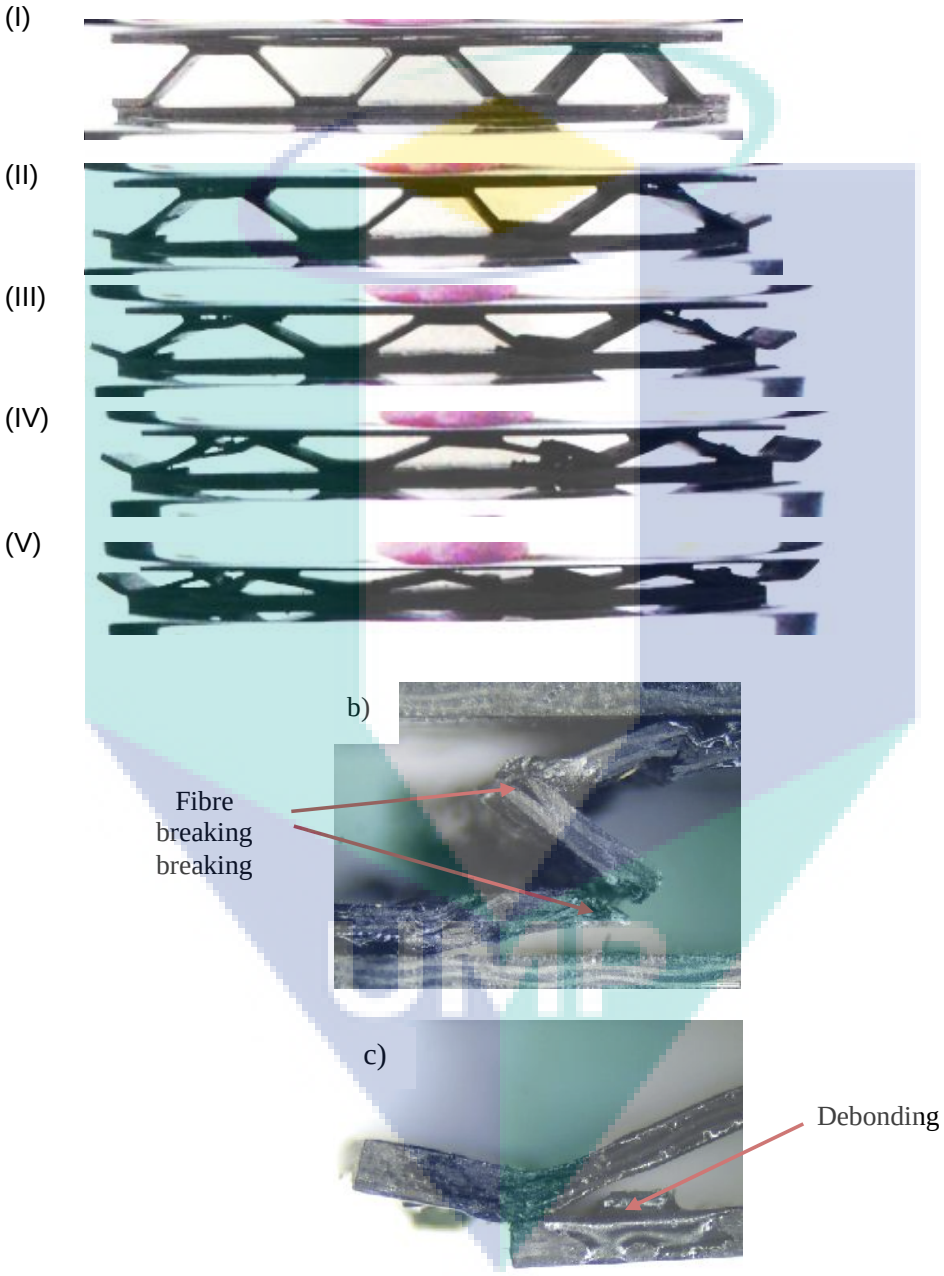

Figure 4.9: a) Photograph of compression behaviour of CFRP trapezoidal corrugated-core based on three unit cells b) Fracture after the corrugated-core has been almost completely flattened (a)-V). c) Debonding at the end of the core after compression

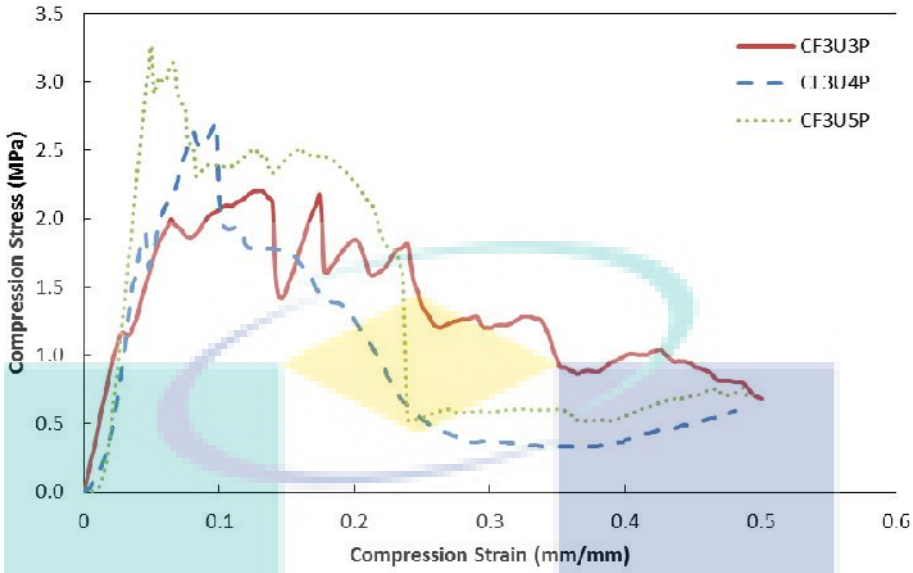

Figure 4.10: Comparison of Stress-Strain Curve on three unit cells CFRP of corrugated-core sandwich structure specimens based on 3, 4 and 5 plies

Figure 4.10 displays that the compression strength increases with increasing of cell wall thickness in the core. As can be seen in Figure 4.10 CF3U5P with 5-ply carbon fibre has the highest compression stress which is 3.25 MPa. During the experiment, the thickest core (CF3U5P) exhibited a combination of fracture mechanisms immediately after the sudden load drop from the compression test, as the composite layers delaminated and the edges of the specimen debonded.

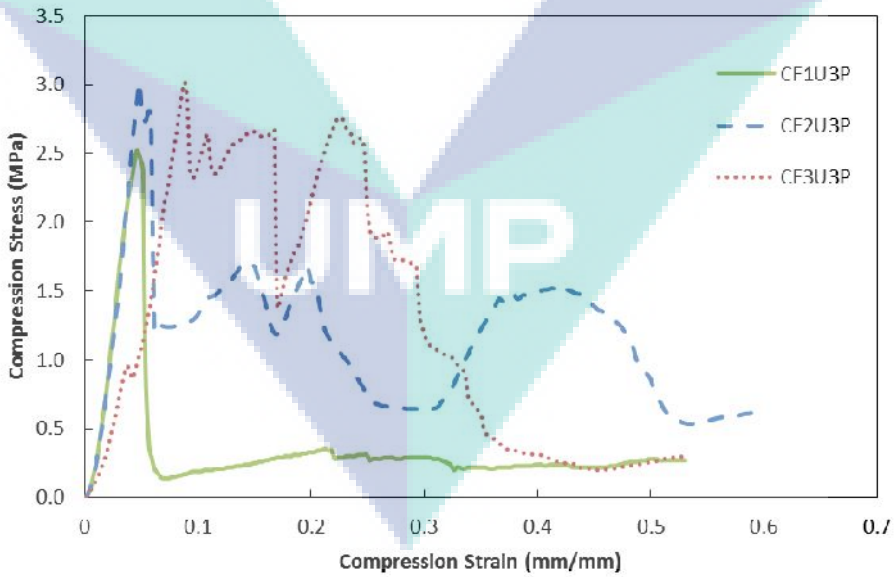

Figure 4.11: Comparison of Load-Displacement Curve for CFRP of corrugated-core sandwich structure specimens based on 1, 2 and 3 unit cells. These are specimens of 3 plies thickness

Figure 4.11 shows the compression responses of the CFRP trapezoidal corrugated-core sandwich structure specimens. Based on these observations, it shows that, right

just after the peak load, the fibres start to fracture, and the crushing process continues until compressed region. With an increase in the number of unit cells, the compression loads increase drastically. For specimen CF2U3P and CF3U3P, it has nearest similar peak. This is because for 2U (2 unit) and 3U (3 unit), it is because of the vertical structure that supports the trapezoidal structure. From Figure 4.11 the curve shows three patterns that reflect to the number of unit itself. For example, CF1U3P has only one peak and the compression stress increase drastically, then drops at 2.5 MPa and flat until the end of compression while for CF3U3P, there are three peaks. Table 4.1 tabulates a summary of CFRP corrugated-core sandwich structure under compression test. Maximum load was dominated by specimen CF3U5P_S3 (carbon fibre with three-unit cell and five plies, specimen 3) with 11.69 kN and compression strength 3.89 MPa.

Table 4.1: Summary of CFRP corrugated-core sandwich structure under compression test

Core ID	Maximum Load, P (kN)	Compression Strength, σ (MPa)	Compression Strain, ε (mm/mm) at compression strength
CF1U3P_S1	1.97	1.97	0.074
CF1U3P_S2	2.54	2.54	0.053
CF1U3P_S3	1.18	1.18	0.051
CF1U4P_S1	3.16	3.16	0.056
CF1U4P_S2	3.33	3.33	0.042
CF1U4P_S3	0.87	0.87	0.053
CF1U5P_S1	0.88	0.97	0.028
CF1U5P_S2	1.85	1.85	0.033
CF1U5P_S3	0.72	0.78	0.031
CF2U3P_S1	5.72	2.86	0.143
CF2U3P_S2	3.52	1.76	0.052
CF2U3P_S3	5.99	3.04	0.070
CF2U4P_S1	5.34	2.67	0.089
CF2U4P_S2	8.11	4.06	0.219
CF2U4P_S3	3.63	1.82	0.129
CF2U5P_S1	2.66	1.33	0.053
CF2U5P_S2	3.60	1.80	0.038
CF2U5P_S3	4.61	2.31	0.043
CF3U3P_S1	6.61	2.20	0.132
CF3U3P_S2	9.05	3.02	0.088
CF3U3P_S3	4.61	1.54	0.241
CF3U4P_S1	8.53	2.84	0.074
CF3U4P_S2	7.38	2.76	0.070
CF3U4P_S3	8.15	2.72	0.118
CF3U5P_S1	9.78	3.26	0.050
CF3U5P_S2	9.82	3.27	0.042
CF3U5P_S3	11.69	3.89	0.060

The Compression Behaviour of GFRP Corrugated-Core Sandwich Structure

Typically, the load-displacement traces of the GFRP corrugated-core sandwich structures exhibited a brittle type of behaviour, involving extensive crushing as shown in Figure 4.12.

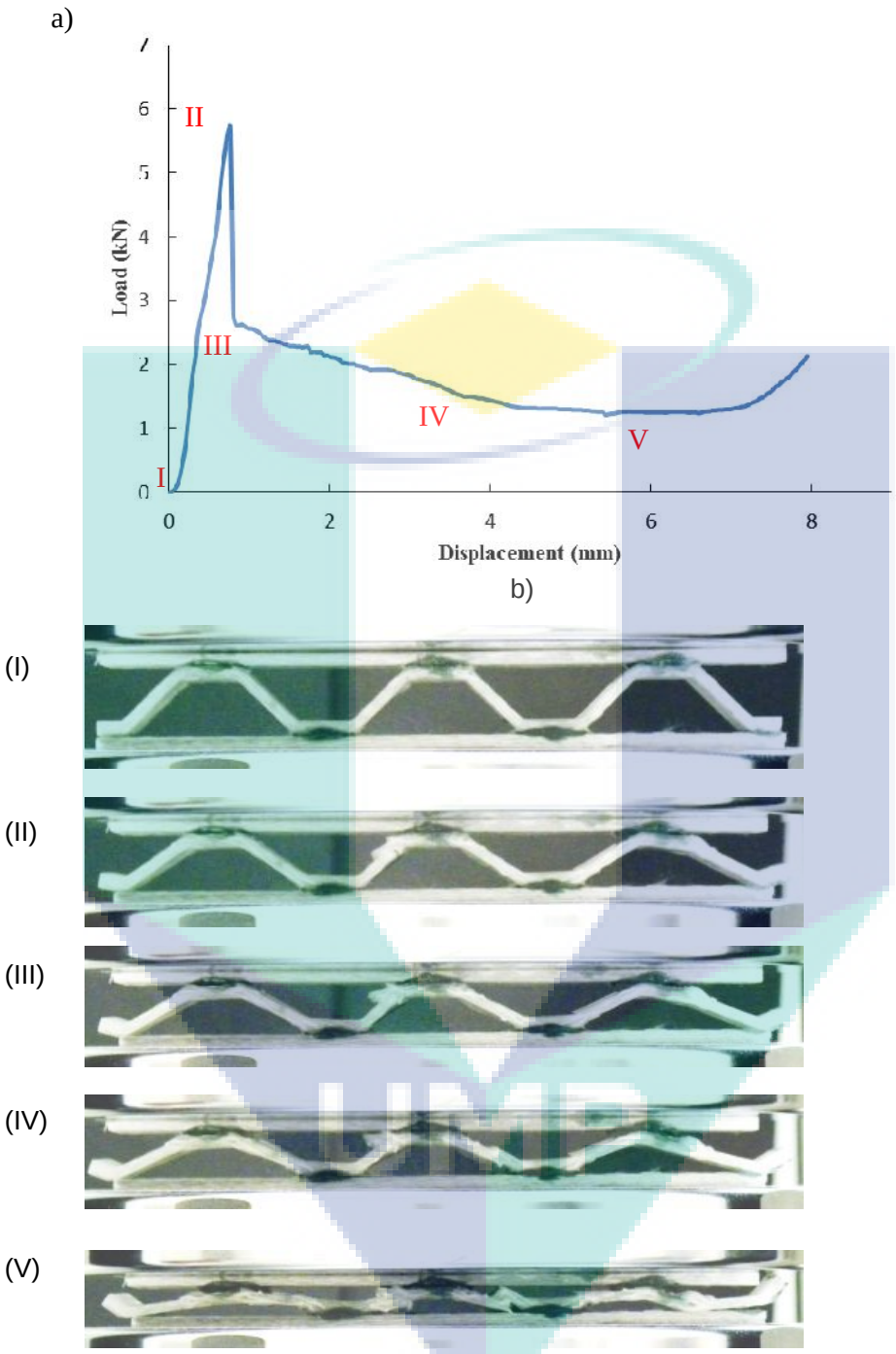

Figure 4.12: a)Load-Displacement Curve of GFRP in compression. b)Compression behaviour of GFRP trapezoidal corrugated-core

Figure 4.12(a) shows graph of a load-displacement curve of three-unit cell corrugated core sandwich structure with three plies. The failure processes in GFRP trapezoidal corrugated-core are shown in Figure 4.12(b), the initial failure start with debonding at the end of right and left specimen followed by sudden break at II thus cause the compression stress to decrease and the strut starts to have fracture at III in the unit cell

and continue decrease until the compression test stop. Following failures include delamination, fibre breaking and debonding (III-V).

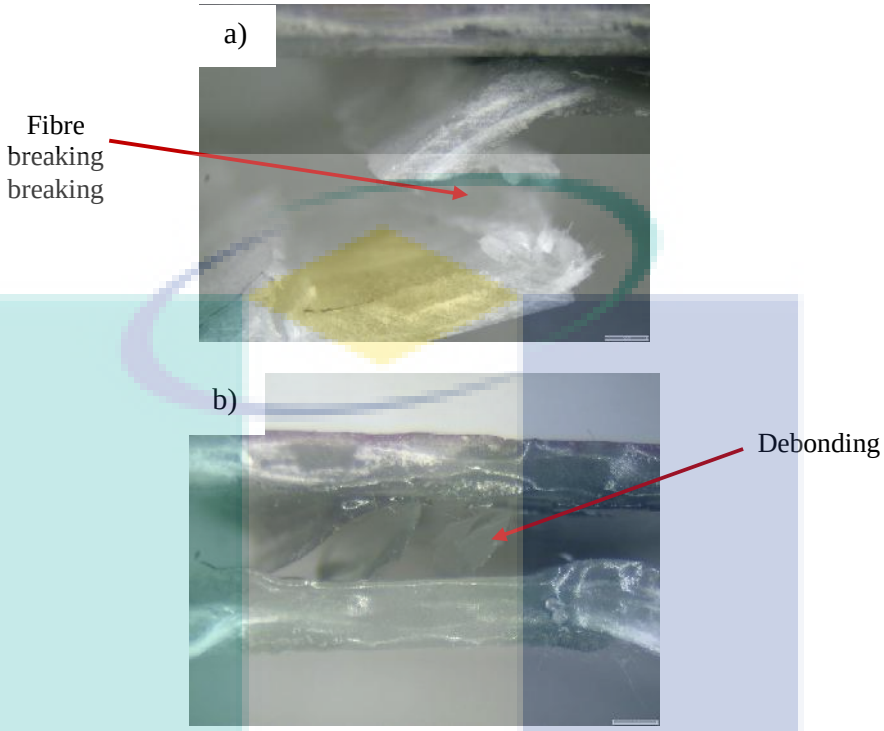

Figure 4.13: Photograph of compression behaviour of GFRP trapezoidal corrugated-core based on three unit cells a) Fracture after the corrugated-core has been almost completely flattened b) Debonding at the core after compression

Figure 4.13 shows photograph of compression behaviour of GFRP trapezoidal corrugated-core based on three-unit cells. a) Fracture after the corrugated-core has been almost completely flattened. b) Debonding at the core after compression. Table 4.2 summaries the properties of GFRP corrugated-core sandwich structure under compression test. From the table, it shows that maximum load was dominated by the highest unit cell and thickness GF3U4P_S3 with 10.17 kN and compression strength 3.39 MPa. It also shows that number of unit cell and thickness of the wall is crucial in sandwich structure construction.

Table 4.2: Summary of GFRP corrugated-core sandwich structure under compression test

Core ID	Max Load, P (kN)	Compression Strength, σ (MPa)	Compression Strain, ε (mm/mm) at compression strength
GF1U2P_S1	0.47	0.45	0.021
GF1U2P_S2	0.76	0.75	0.045
GF1U2P_S3	0.66	0.32	0.070
GF1U3P_S1	1.15	1.15	0.024
GF1U3P_S2	0.58	0.58	0.014
GF1U3P_S3	1.02	1.02	0.012
GF1U4P_S1	1.66	1.66	0.018
GF1U4P_S2	0.99	0.99	0.019
GF1U4P_S3	1.61	1.61	0.014

GF2U2P_S1	**1.86**	**0.92**	**0.082**
GF2U2P_S2	**2.07**	**1.01**	**0.096**
GF2U2P_S3	**2.78**	**1.11**	**0.062**
GF2U3P_S1	**3.17**	**1.58**	**0.028**
GF2U3P_S2	**3.52**	**1.76**	**0.037**
GF2U3P_S3	**3.65**	**1.83**	**0.030**
GF2U4P_S1	**4.67**	**2.33**	**0.030**
GF2U4P_S2	**3.85**	**1.93**	**0.021**
GF2U4P_S3	**3.88**	**1.94**	**0.025**
GF3U2P_S1	**3.57**	**1.19**	**0.115**
GF3U2P_S2	**3.16**	**1.05**	**0.116**
GF3U2P_S3	**2.92**	**0.97**	**0.099**
GF3U3P_S1	**4.94**	**1.65**	**0.045**
GF3U3P_S2	**5.73**	**1.91**	**0.045**
GF3U3P_S3	**3.89**	**1.64**	**0.051**
GF3U4P_S1	**10.06**	**3.35**	**0.039**
GF3U4P_S2	**8.83**	**2.94**	**0.036**
GF3U4P_S3	**10.17**	**3.39**	**0.043**

Effect of Varying Number of Unit Cell and Varying Number of Plies

In attempts to validate more precisely, tests were conducted on three specimens for GFRP and CFRP. The effect of varying number of unit cell and varying wall thickness on compression strength of GFRP and CFRP trapezoidal corrugated-core sandwich structure is shown in Figure 4.14 and Figure 4.15. Obviously, the compression strength of (CFRP) is much higher than GFRP structure due to the fact that carbon fibres have higher mechanical properties than GFRP (Elanchezhian et al., 2014). Carbon Fibre has a high strength-to-weight ratio when tested unidirectionally in the direction of the fibres, while glass fibre has a lower strength-to-weight ratio. Figure 4.14 shows the effect of varying the number of unit cell for GFRP and CFRP from one to three-unit cells. It shows that the higher number of unit cell, it influences the composite strength. For the effect of cell wall thickness, Figure 4.15 shows the higher the wall thickness, the higher the compression strength.

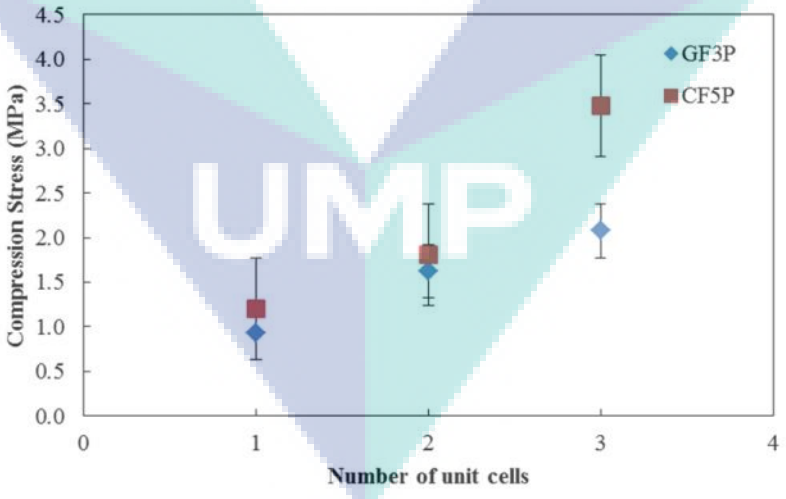

Figure 4.14: Comparison between glass fibre three plies (GF3P) with carbon fibre 5 plies (CF5P)

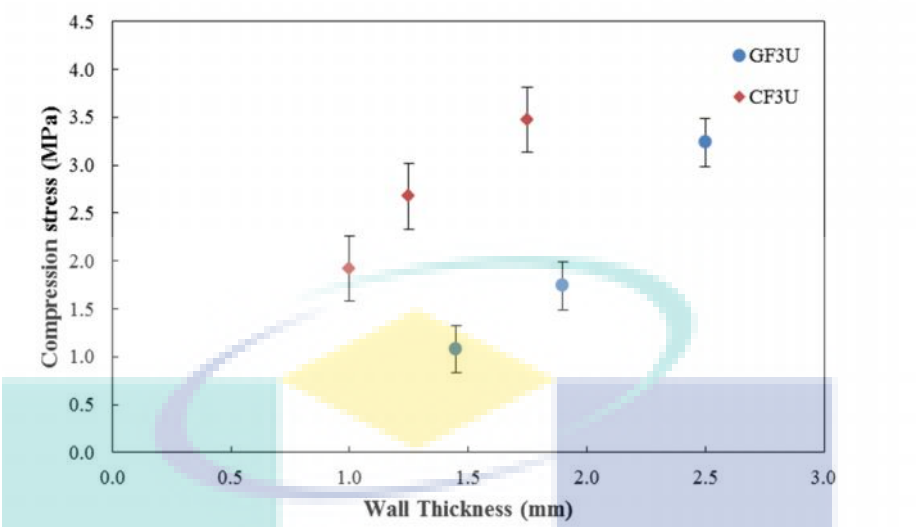

Figure 4.15: Comparison between glass fibre three unit cells (GF3U) and carbon fibre three unit cell (CF3U) with different wall thicknesses

Static Tensile Test for Corrugated-core Structure

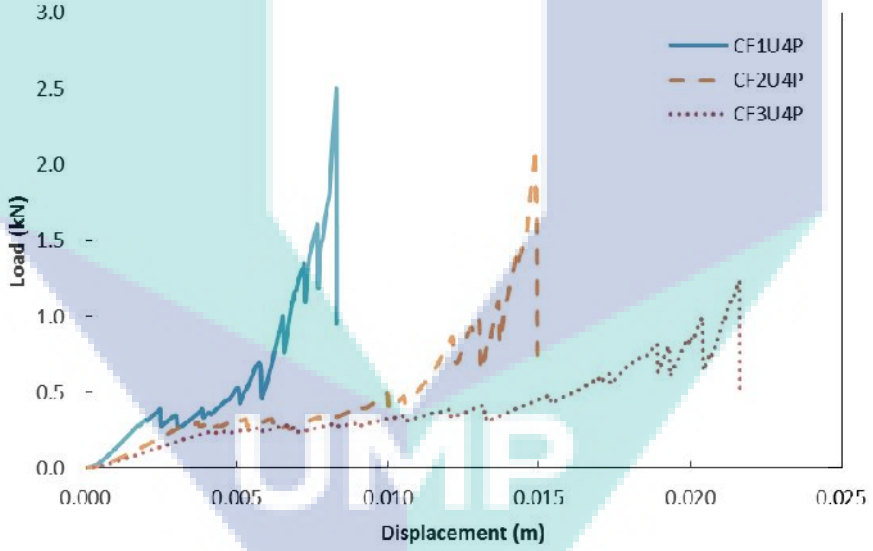

Figure 4.16: Static tensile Load-Displacement Curve of corrugated-core with four plies

Figure 4.16 and Figure 4.17 show the tension responses and stress strain curve of CFRP trapezoidal corrugated-core specimens based on 1, 2 and 3-unit cells. The graph shows with the increase of unit cell, the extension also increase. This is because, the presence of fibre wave in woven fabrics as the fibre yarns in the fill direction cross over and under the fibre yarns in the warp direction to create an interlocked structure. In tensile loading, these wavy fibres be likely straighten out, which creates high stresses in the matrix. Consequently, micro cracks occur in the matrix at relatively low loads (Mallick, 2007). CFRP structure with single unit cell has lower extension than CFRP structure with three (3) unit cell. As a result, one-unit cell has structure with two vertical beams, when the tension occurs.

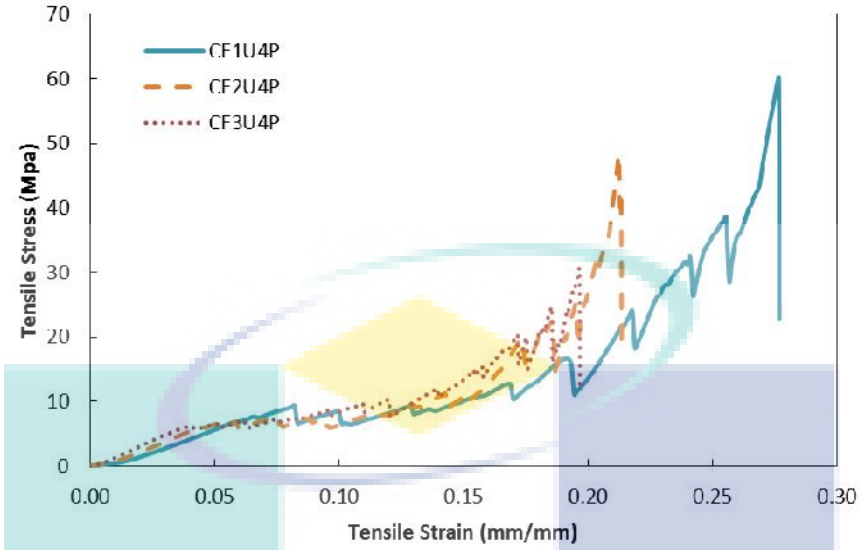

Figure 4.17: Stress-Strain Curve static corrugated-core for tensile test for four plies

a)

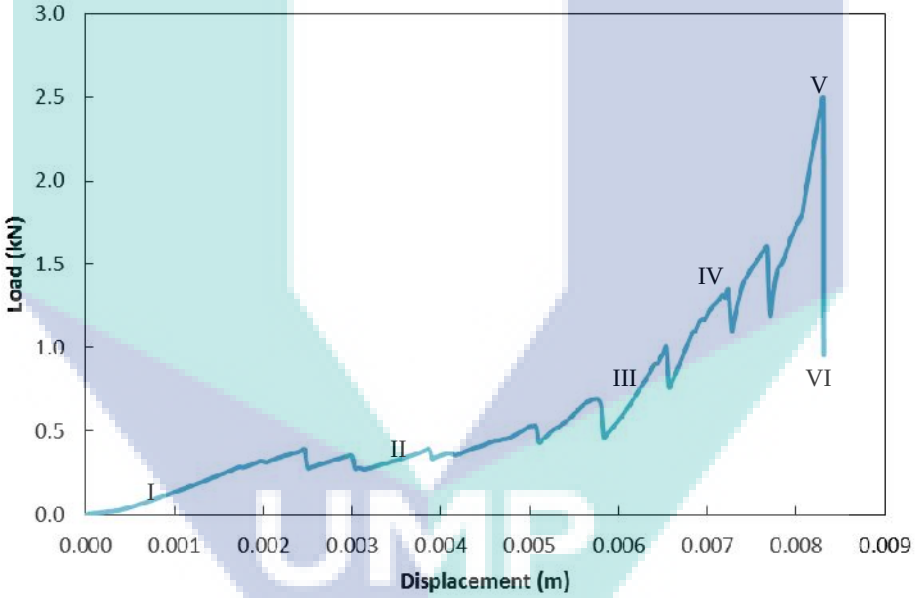

b)

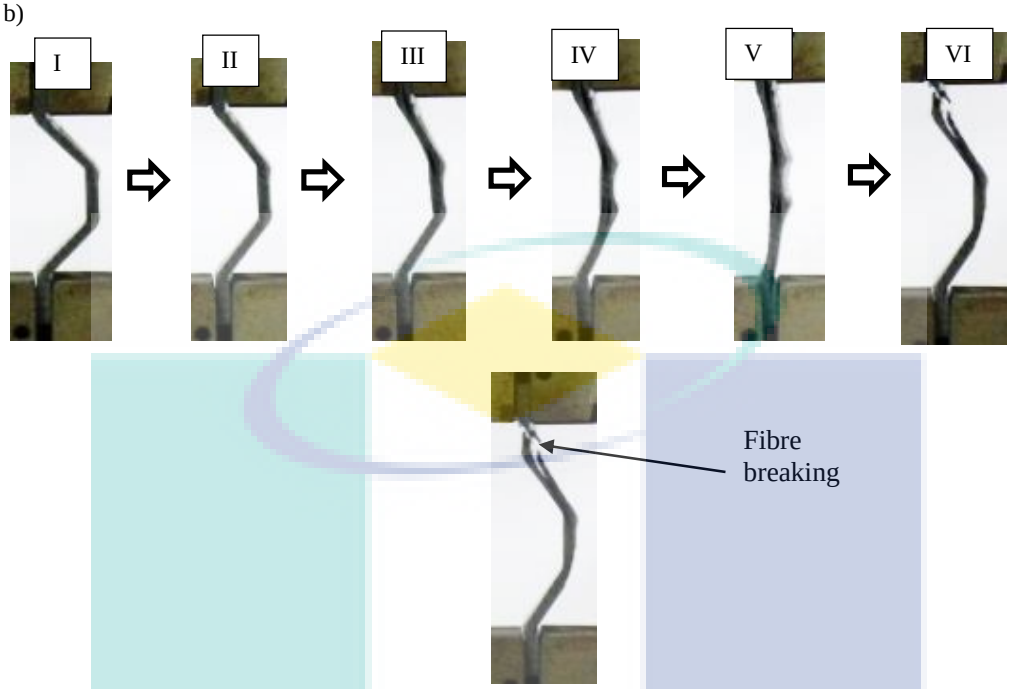

Figure 4.18: a) Load-Displacement Curve of CFRP in tension. b) Corrugated specimen behaviour in tensile test

Figure 4.18 shows a) load-displacement curve and b) behaviour of trapezoidal corrugated-core with one-unit cell in tensile test. The test was conducted using cross speed 2mm/min. The graph increase gradually at (I-II) and increase drastically at III-IV when the elongation starts to increase. When the microfibre starts to cracking and give fibre cracking sound. At V the corrugated-core structure start to straighten out which creates high stresses in the matrix. Fibre break at VI, the figure shows fibre break at edges of the corrugated-core, this might be because of the matrix at the top edges start to break first and cause the fibre at the edges to cracking and break. The maximum tensile load reached to 2.5 kN at 0.0083 m.

Validation between Experimental Result and Numerical Data

Simulation for compression is performed to understand the compression behaviour and to validate between experiment and finite element analysis. Table 4.3 shows displacement and behaviour of corrugated-core in compression in both experiment and simulation. Compression behaviour for experiment and FEM shows significant comparable.

Table 4.3: Displacement and behaviour of corrugated-core in compression

Load, Displacement	Experimental	Finite Element Analysis
0 mm 0kN		
1.0 mm 7.46kN	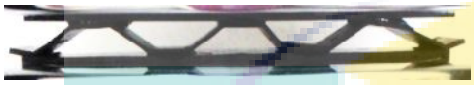	
2.0 mm 7.89kN	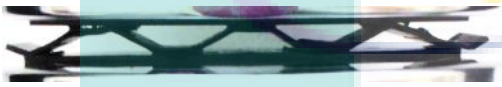	
3.0 mm 8.03kN		
4.0 mm 3.25kN	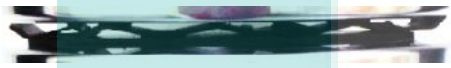	

It should be noted that for the initial numerical predictions, based on FE-Perfect model, the predicted peak load and stiffness are higher for all types of composites corrugation. From the imperfection-sensitivity method and the analysis data, an initial imperfection with amplitude of 0.03 was introduced into both of the GFRP and CFRP models. Following this, the comparison between the numerical and experimental results was reasonably good. It is evident that the numerical models for of the GFRP and CFRP corrugations fails to predict the early instabilities in the load-displacement trace. Beyond peak load, the CFRP over-predicts the softening phase of the deformation process. This occurs due to Abaqus/Standard being unable to eliminate the failed elements, giving over predictions of the behaviour. Element deletion can only be activated in Abaqus/Explicit. The predicted deformation mode is presented and compared with the experimental deformation mode in Table 4.3. The figure also highlighting good agreement in terms of failure mode shapes.

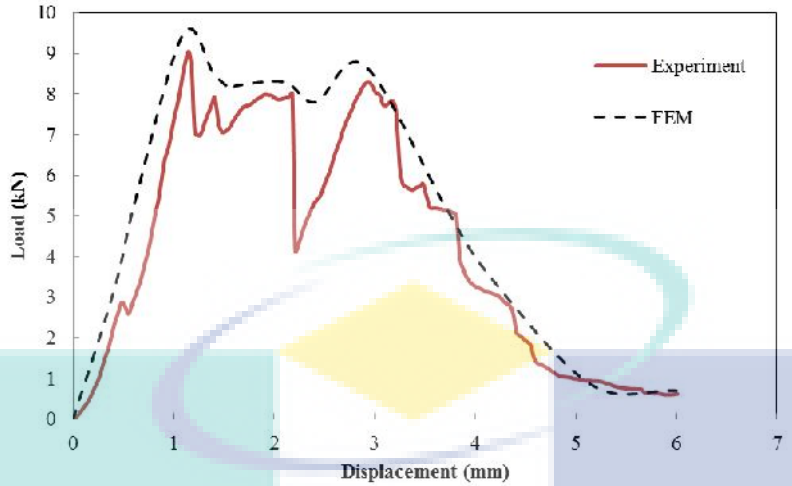

Figure 4.19: Validation between FE result and experimental data. FE simulation for CFRP with ξ = 0.03 show reasonable agreement with the measured response

As can be seen in Figure 4.19, a very good agreement is found between experimental and finite element values. A percentage error calculation simply tells the magnitude of the mistakes that took place during the experiment. This observation is validated by computing the percentage errors between finite element and average experimental results with discrepancy around 4.97% in maximum load as shown in Table 4.4.

$$\%_{error} = \frac{FE - Exp}{Exp} \times 100\% \quad 4.1$$

$$\%_{error} = \frac{9.50 - 9.05}{9.05} \times 100\% = 4.97\% \quad 4.2$$

Table 4.4: Percentage error between experiment and finite element analysis

Analysis	Experiment	Finite Element	Percentage Error (%)
Maximum Load (kN)	**9.05**	**9.5**	**4.97%**

5. CONCLUSION

1. *To investigate the behaviour of trapezoidal corrugated-core subjected to tension and compression loading.*

Compression tests were carried out to determine the compression strength and stiffness of the specimens under compression loading. The compression behaviour starts with debonding at the end of right and left specimen followed by sudden break, following failure include delamination, fibre breaking and debonding. For tensile test, the tests were carried out to study the tensile strength of the specimens under tension loading.

2. *To model with the mechanical response of trapezoidal corrugated-core sandwich structures in Finite Element software.*

The mechanical properties under static compression, such as compression strength and stiffness have been recorded for each trapezoidal corrugated-core sandwich specimen. The structures shown excellent repeatability in terms of their mechanical response. The mechanical response in compression increases with specimen thickness. A very good agreement can be observed between experimental and finite element values. This observation is validated by computing the percentage errors between finite element and average experimental results with discrepancy around 4.97% for maximum load.

3. *To study the effect of varying the geometrical parameters and properties of the corrugated-cores.*

Varying the number of unit cells, cell wall thickness and widths have a significant influence on the compression behaviour of the corrugated-core sandwich structures. The compression strength and stiffness relatively increases with increasing numbers of unit cell and cell wall thickness. The compressive behaviour and resulting failure mechanism in structures based on two different materials have been investigated experimentally. An investigation of corrugation during testing indicate that initial failure was dominated by instabilities as the cell walls begin to buckle. In contrast, the composite fibre exhibited fibre fracture, delamination and debonding. From the finding, the effects of varying the number of unit cell dominate by CFRP is higher than that GFRP, 2.08 MPa at three-unit cell. It shows that the higher number of unit cell, it influences the composite strength. For the effect of cell wall thickness, it shows the higher the wall thickness, the higher the compression strength. Compression strength CFRP and GFRP are 3.48 MPa and 1.74 MPa at thickness 1.75 mm and 1.90 mm respectively.

ACHIEVEMENT

i) Name of articles/ manuscripts/ books published

a. N.Z.M.Zaid, M.R.M.Rejab, A.F.Jusoh, D.Bachtiar, J.P.Siregar. 2017. Effect of varying geometrical parameters of trapezoidal corrugated-core sandwich structure. *MATEC,* 90, 01018

b. N. Z. M. Zaid, M.R.M. Rejab and N.A.N Mohamed. 2016. Sandwich structure based on corrugated-core: A review. *MATEC.,* 74, 00029

c. A.F.Jusoh, M.R.M. Rejab and D. Bachtiar, J.P. Siregar, 2016. Natural fiber reinforced composites: A review on potential for corrugated core of sandwich structures. *MATEC,* 74, 00033

d. N.Z.M. Zaid, M.R.M. Rejab, A.F. Jusoh, D. Bachtiar, J.P. Siregar, and Zhang Dian-ping. 2016. Fracture Behaviours in Compression-loaded Triangular Corrugated Core Sandwich Panels. *MATEC,* 78, 01041

e. M.R.M.Rejab, N.Z.M. Zaid, J.P. Siregar and D. Bachtiar. Scaling effects for Compression Loaded of Corrugated-core Sandwich Panels. 2014. *Advanced Materials Research,* 1133, 241-245

ii) Title of Paper presentations (international/ local)

a. M.R.M.Rejab, D.Bachtiar, J.P.Siregar, P.Paruka, S.H.S.M.Fadzullah, B. Zhang and W.J.Cantwell. "The mechanical behaviour of foam-filled corrugated core sandwich panels in lateral compression". *31st Technical Conference and ASTM D30 Meeting, American Society for Composites, September 19-22, 2016; Virginia, USA.*

b. N.Z.M.Zaid, M.R.M.Rejab, A.F.Jusoh, D.Bachtiar, J.P.Siregar. "Effect of varying geometrical parameters of trapezoidal corrugated-core sandwich structure". *Automotive Innovation Green Energy Vehicle (AiGeV2016), August 01-02, 2016, Cyberjaya, Kuala Lumpur*

c. N.Z.M. Zaid, M.R.M. Rejab, A.F. Jusoh, D. Bachtiar, J.P. Siregar, and Zhang Dian-ping. "Fracture behaviours in compression-loaded triangular corrugated core sandwich panels". *The International Conference on Green Design and Manufacture (IConGDM 2016), May 01-02, 2016; Phuket, Thailand.*

d. N. Z. M. Zaid, M.R.M. Rejab and N.A.N Mohamed. "Sandwich structure based on corrugated-core: A review". *3rd International Conference on Mechanical Engineering Research (ICMER2015), August 01-02, 2015; Kuantan, Pahang*

e. A.F.Jusoh, M.R.M. Rejab and D. Bachtiar, J.P. Siregar. "Natural fiber reinforced composites: A review on potential for corrugated core of sandwich structures". *3rd International Conference on Mechanical Engineering Research (ICMER2015), August 01-02, 2015; Kuantan, Pahang*

f. M.R.M.Rejab, S.H.S.M.Fadzullah, K.A.Kamarudin, F.Mat. "Numerical Modelling of Triangular Corrugated-core Sandwich Panel subjected to Impact Loading". *Malaysian Technical Universities Conference on Engineering & Technology (MUCET2014), November 10-11, 2014; Melaka.*

iii) Human Capital Development

Two masters students:

a. NOOR ZAKIAH BINTI MD ZAID - 871119026210 - (MMM14038)
b. AHMAD FAHMY BIN JUSOH - 860715335403 - (MMM14045)

Four Undergraduate students:

a. MUHAMMAD NUR ARIFF HAKIMI MOHD JAAFAR (MB12129)
b. NURKHALEEDA BINTI ROMLI (MC12017)
c. MOHD SYAFIQ BIN ABDUL JALIL (MA11145)
d. NUR DINA BINTI SUHAIMI (MG12011)

iv) Awards/ Others

Nil

v) Others

Nil

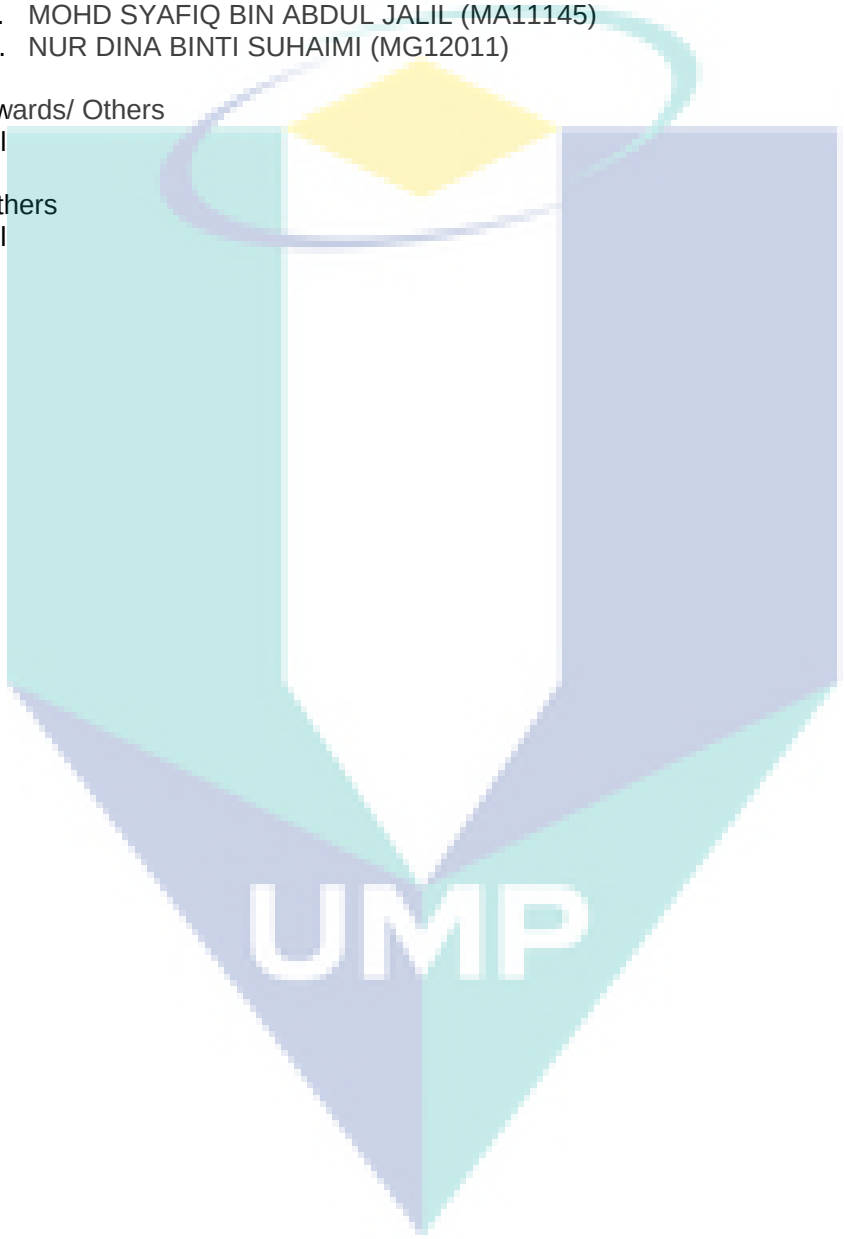

REFERENCES

Abbadi, A., Koutsawa, Y., Carmasol, a., Belouettar, S., & Azari, Z. (2009). Experimental and numerical characterization of honeycomb sandwich composite panels. *Simulation Modelling Practice and Theory*, *17*(10), 1533–1547. http://doi.org/10.1016/j.simpat.2009.05.008

Aktay, L., Johnson, A. F., & Kröplin, B.-H. (2008). Numerical modelling of honeycomb core crush behaviour. *Engineering Fracture Mechanics*, *75*(9), 2616–2630. http://doi.org/10.1016/j.engfracmech.2007.03.008

Bartolozzi, G., Baldanzini, N., & Pierini, M. (2014). Equivalent properties for corrugated cores of sandwich structures: A general analytical method. *Composite Structures*, *108*(1), 736–746. http://doi.org/10.1016/j.compstruct.2013.10.012

Bartolozzi, G., Baldanzini, N., Pierini, M., & Zonfrillo, G. (2015). Static and dynamic experimental validation of analytical homogenization models for corrugated core sandwich panels. *Composite Structures*, *125*, 343–353. http://doi.org/10.1016/j.compstruct.2015.02.014

Bartolozzi, G., Pierini, M., Orrenius, U., & Baldanzini, N. (2013). An equivalent material formulation for sinusoidal corrugated cores of structural sandwich panels. *Composite Structures*, *100*, 173–185. http://doi.org/10.1016/j.compstruct.2012.12.042

Belingardi, G., Martella, P., & Peroni, L. (2007). Fatigue analysis of honeycomb-composite sandwich beams. *Composites Part A: Applied Science and Manufacturing*, *38*(4), 1183–1191. http://doi.org/10.1016/j.compositesa.2006.06.007

Belouettar, S., Abbadi, a., Azari, Z., Belouettar, R., & Freres, P. (2009). Experimental investigation of static and fatigue behaviour of composites honeycomb materials using four point bending tests. *Composite Structures*, *87*(3), 265–273. http://doi.org/10.1016/j.compstruct.2008.01.015

Bin, H., Bo, Y., Yu, X., Chang-Qing, C., Qian-Cheng, Z., & Tian Jian, L. (2015). Foam filling radically enhances transverse shear response of corrugated sandwich plates. *Materials and Design*, *77*, 132–141. http://doi.org/10.1016/j.matdes.2015.03.050

Bisagni, C. (2000). Numerical analysis and experimental correlation of composite shell buckling and post-buckling. *Composites Part B: Engineering*, *31*(8), 655–667. http://doi.org/10.1016/S1359-8368(00)00031-7

Buannic, N., Cartraud, P., & Quesnel, T. (2003). Homogenization of corrugated core sandwich panels. *Composite Structures*, *59*(3), 299–312. http://doi.org/10.1016/S0263-8223(02)00246-5

Burlayenko, V. N., & Sadowski, T. (2009). Analysis of structural performance of sandwich plates with foam-filled aluminum hexagonal honeycomb core. *Computational Materials Science*, *45*, 658–662. http://doi.org/10.1016/j.commatsci.2008.08.018

Burman, M., & Zenkert, D. (1997). Fatigue of foam core sandwich beams—1: undamaged specimens. *International Journal of Fatigue*, *19*(7), 551–561. http://doi.org/10.1016/S0142-1123(97)00069-8

Chang, W., Ventsel, E., Krauthammer, T., & John, J. (2005). Bending behavior of

corrugated-core sandwich plates, *70*, 81–89. http://doi.org/10.1016/j.compstruct.2004.08.014

Che, L., Xu, G. D., Zeng, T., Cheng, S., Zhou, X. W., & Yang, S. C. (2014). Compressive and shear characteristics of an octahedral stitched sandwich composite. *Composite Structures*, *112*(1), 179–187. http://doi.org/10.1016/j.compstruct.2014.02.012

Chen, C., Harte, A. M., & Fleck, N. A. (2001). Plastic collapse of sandwich beams with a metallic foam core. *International Journal of Mechanical Sciences*, *43*, 1483–1506. http://doi.org/10.1016/S0020-7403(00)00069-2

Choi, H. S., & Jang, Y. H. (2010). Bondline strength evaluation of cocure/precured honeycomb sandwich structures under aircraft hygro and repair environments. *Composites Part A: Applied Science and Manufacturing*, *41*(9), 1138–1147. http://doi.org/10.1016/j.compositesa.2010.04.012

Côté, F., Deshpande, V. S., Fleck, N. A., & Evans, A. G. (2006). The compressive and shear responses of corrugated and diamond lattice materials. *International Journal of Solids and Structures*, *43*, 6220–6242. http://doi.org/10.1016/j.ijsolstr.2005.07.045

Crupi, V., & Montanini, R. (2007). Aluminium foam sandwiches collapse modes under static and dynamic three-point bending. *International Journal of Impact Engineering*, *34*(3), 509–521. http://doi.org/10.1016/j.ijimpeng.2005.10.001

Dayyani, I., Ziaei-rad, S., & Salehi, H. (2012). Numerical and Experimental Investigations on Mechanical Behavior of Composite Corrugated Core, 705–721. http://doi.org/10.1007/s10443-011-9238-3

Dayyani, I., Ziaei-Rad, S., & Salehi, H. (2011). Numerical and Experimental Investigations on Mechanical Behavior of Composite Corrugated Core. *Applied Composite Materials*, *19*(3–4), 705–721. http://doi.org/10.1007/s10443-011-9238-3

Elanchezhian, C., Ramnath, B. V., & Hemalatha, J. (2014). Mechanical Behaviour of Glass and Carbon Fibre Reinforced Composites at Varying Strain Rates and Temperatures. *Procedia Materials Science*, *6*, 1405–1418. http://doi.org/10.1016/j.mspro.2014.07.120

Evans, A. G., Hutchinson, J. W., Fleck, N. A., Ashby, M. F., & Wadley, H. N. G. (2001). The topological design of multifunctional cellular metals. In *Progress in Materials Science* (Vol. 46, pp. 309–327). http://doi.org/10.1016/S0079-6425(00)00016-5

Foo, C. C., Chai, G. B., & Seah, L. K. (2007). Mechanical properties of Nomex material and Nomex honeycomb structure. *Composite Structures*, *80*(4), 588–594. http://doi.org/10.1016/j.compstruct.2006.07.010

Frank Xu, X., & Qiao, P. (2002). Homogenized elastic properties of honeycomb sandwich with skin effect. *International Journal of Solids and Structures*, *39*(8), 2153–2188. http://doi.org/10.1016/S0020-7683(02)00111-7

George, T., Deshpande, V. S., Sharp, K., & Wadley, H. N. G. (2014). Hybrid core carbon fiber composite sandwich panels: Fabrication and mechanical response. *Composite Structures*, *108*(1), 696–710. http://doi.org/10.1016/j.compstruct.2013.10.002

Grujicic, M., Galgalikar, R., Snipes, J. S., Yavari, R., & Ramaswami, S. (2013). Multi-physics modeling of the fabrication and dynamic performance of all-metal auxetic-hexagonal sandwich-structures. *Materials and Design*, *51*, 113–130. http://doi.org/10.1016/j.matdes.2013.04.004

Han, B., Qin, K., Yu, B., Zhang, Q., Chen, C., & Jian, T. (2015). Design optimization of foam-reinforced corrugated sandwich beams, *130*, 51–62. http://doi.org/10.1016/j.compstruct.2015.04.022

Harte, A., Fleck, N. A., & Ashby, M. F. (2001). The fatigue strength of sandwich beams with an aluminium alloy foam core, *23*, 499–507.

He, C., Chen, J., Wu, Z., Xie, J., Zu, Q., & Lu, Y. (2015). Simulated effect on the compressive and shear mechanical properties of bionic integrated honeycomb plates. *Materials Science & Engineering C*, *50*, 286–293. http://doi.org/10.1016/j.msec.2015.02.011

He, M., & Hu, W. (2008). A study on composite honeycomb sandwich panel structure. *Materials & Design*, *29*(3), 709–713. http://doi.org/10.1016/j.matdes.2007.03.003

He, W., Liu, J., Tao, B., Xie, D., Liu, J., & Zhang, M. (2016). Experimental and numerical research on the low velocity impact behavior of hybrid corrugated core sandwich structures. *Composite Structures*, *158*, 30–43. http://doi.org/10.1016/j.compstruct.2016.09.009

Heimbs, S. (2009). Virtual testing of sandwich core structures using dynamic finite element simulations. *Computational Materials Science*, *45*, 205–216. http://doi.org/10.1016/j.commatsci.2008.09.017

Hou, S., Shu, C., Zhao, S., Liu, T., Han, X., & Li, Q. (2015). Experimental and numerical studies on multi-layered corrugated sandwich panels under crushing loading. *Composite Structures*, *126*, 371–385. http://doi.org/10.1016/j.compstruct.2015.02.039

Hou, S., Zhao, S., Ren, L., Han, X., & Li, Q. (2013). Crashworthiness optimization of corrugated sandwich panels. *Materials and Design*, *51*, 1071–1084. http://doi.org/10.1016/j.matdes.2013.04.086

Hu, Y., Li, W., An, X., & Fan, H. (2016). Fabrication and mechanical behaviors of corrugated lattice truss composite sandwich panels. *Composites Science and Technology*, *125*, 114–122. http://doi.org/10.1016/j.compscitech.2016.02.003

Isaksson, P., Krusper, A., & Gradin, P. A. (2007). Shear correction factors for corrugated core structures, *80*, 123–130. http://doi.org/10.1016/j.compstruct.2006.04.066

Ivañez, I., Santiuste, C., & Sanchez-Saez, S. (2010). FEM analysis of dynamic flexural behaviour of composite sandwich beams with foam core. *Composite Structures*, *92*, 2285–2291. http://doi.org/10.1016/j.compstruct.2009.07.018

Jen, Y., & Chang, L. (2008). Evaluating bending fatigue strength of aluminum honeycomb sandwich beams using local parameters. *International Journal of Fatigue*, *30*(6), 1103–1114. http://doi.org/10.1016/j.ijfatigue.2007.08.006

Kazemahvazi, S., Tanner, D., & Zenkert, D. (2009). Corrugated all-composite sandwich structures . Part 2: Failure mechanisms and experimental programme. *Composites Science and Technology*, *69*(7–8), 920–925. http://doi.org/10.1016/j.compscitech.2008.11.035

Kazemahvazi, S., & Zenkert, D. (2009). Corrugated all-composite sandwich structures. Part 1: Modeling. *Composites Science and Technology*, *69*, 913–919. http://doi.org/10.1016/j.compscitech.2008.11.030

Kesler, O., & Gibson, L. . (2002). Size effects in metallic foam core sandwich beams. *Materials Science and Engineering: A*, *326*(2), 228–234. http://doi.org/10.1016/S0921-5093(01)01487-3

Kiliçaslan, C., Güden, M., Odaci, I. K., & Taşdemirci, A. (2013). The impact responses and the finite element modeling of layered trapezoidal corrugated aluminum core and aluminum sheet interlayer sandwich structures. *Materials and Design*, *46*, 121–133. http://doi.org/10.1016/j.matdes.2012.09.059

Kiliçaslan, C., Güden, M., Odaci, I. K., & Taşdemirci, A. (2014). Experimental and numerical studies on the quasi-static and dynamic crushing responses of multi-layer trapezoidal aluminum corrugated sandwiches. *Thin-Walled Structures*, *78*, 70–78. http://doi.org/10.1016/j.tws.2014.01.017

Konka, H. P., Wahab, M. a., & Lian, K. (2012). On Mechanical Properties of Composite Sandwich Structures With Embedded Piezoelectric Fiber Composite Sensors. *Journal of Engineering Materials and Technology*, *134*(1), 11010. http://doi.org/10.1115/1.4005349

Kooistra, G. W., & Wadley, H. N. G. (2007). Hierarchical Corrugated Core Sandwich Panel Concepts, *74*(March). http://doi.org/10.1115/1.2198243

Li, C., Ueno, R., & Lefebvre, V. (2006). Investigation of an Accelerated Moisture Removal Approach of a Composite Aircraft Control Surface. *Society for the Advancement,* Retrieved from http://people.physics.carleton.ca/~rueno/files/ge_lic.pdf

Lim, J. Y., & Bart-Smith, H. (2015). An analytical model for the face wrinkling failure prediction of metallic corrugated core sandwich columns in dynamic compression. *International Journal of Mechanical Sciences*, *92*, 290–303. http://doi.org/10.1016/j.ijmecsci.2015.01.002

Lim, J. Y., & Bart-Smith, H. (2016). High velocity compressive response of metallic corrugated core sandwich columns. *International Journal of Mechanical Sciences*, *106*, 78–94. http://doi.org/10.1016/j.ijmecsci.2015.12.010

Magnucka-blandzi, E., Magnucki, K., & Wittenbeck, L. (2015). Mathematical modeling of shearing effect for sandwich beams with sinusoidal corrugated cores. *Applied Mathematical Modelling*, *39*(9), 2796–2808. http://doi.org/10.1016/j.apm.2014.10.069

Magnucki, K., Magnucka-Blandzi, E., & Wittenbeck, L. (2014). Elastic bending and buckling of a steel composite beam with corrugated main core and sandwich faces-Theoretical study. *Applied Mathematical Modelling*, *40*(2), 1276–1286. http://doi.org/10.1016/j.apm.2015.06.035

Malcom, A. J., Aronson, M. T., Deshpande, V. S., & Wadley, H. N. G. (2013).

Composites : Part A Compressive response of glass fiber composite sandwich structures. *Composites Part A*, *54*, 88–97. http://doi.org/10.1016/j.compositesa.2013.07.007

Mallick, P. K. (2007). *Fiber- Reinforced Composites* (Third). Michigan: Taylor & Francis Group.

McElroy, M., Leone, F., Ratcliffe, J., Czabaj, M., & Yuan, F. G. (2015). Simulation of delamination-migration and core crushing in a CFRP sandwich structure. *Composites Part A: Applied Science and Manufacturing*, *79*, 192–202. http://doi.org/10.1016/j.compositesa.2015.08.026

Mohammadi, H., Ziaei-Rad, S., & Dayyani, I. (2015). An equivalent model for trapezoidal corrugated cores based on homogenization method. *Composite Structures*, *131*, 160–170. http://doi.org/10.1016/j.compstruct.2015.04.048

Mohan, K., Yip, T. H., Idapalapati, S., & Chen, Z. (2011). Impact response of aluminum foam core sandwich structures. *Materials Science and Engineering A*, *529*, 94–101. http://doi.org/10.1016/j.msea.2011.08.066

Petras, A., & Sutcliffe, M. P. F. (1999). Failure mode maps for honeycomb sandwich panels. *Composite Structures*, *44*, 237–252.

Pora, J. (2001). Composite Materials in the Airbus A380 - From History to Future -. *Proceedings ICCM-13*, 1–10.

Reany, J., & Grenestedt, J. L. (2009). Corrugated skin in a foam core sandwich panel. *Composite Structures*, *89*(3), 345–355. http://doi.org/10.1016/j.compstruct.2008.08.008

Rejab, M. R. M., & Cantwell, W. J. (2013). The mechanical behaviour of corrugated-core sandwich panels. *Composites Part B: Engineering*, *47*, 267–277. http://doi.org/10.1016/j.compositesb.2012.10.031

Rejab, M. R. M., Hassan, W. a. W., Siregar, J. P., & Bachtiar, D. (2014). Specific Properties of Novel Two-Dimensional Square Honeycomb Composite Structures. *Applied Mechanics and Materials*, *695*, 694–698. http://doi.org/10.4028/www.scientific.net/AMM.695.694

Rejab, M. R. M., Zaid, N. Z. M., Siregar, J. P., & Bachtiar, D. (2016). Scaling Effects for Compression Loaded of Corrugated-Core Sandwich Panels. *Advanced Materials Research*, *1133* (November), 241–245. http://doi.org/10.4028/www.scientific.net/AMR.1133.241

Rizov, V. I. (2006). Elastic–plastic response of structural foams subjected to localized static loads. *Materials & Design*, *27*(10), 947–954. http://doi.org/10.1016/j.matdes.2005.02.013

Saarimäki, E., & Ylinen, P. (2008). An investigation of non-destructive thermographic inspection exploiting phase transition of water for moisture detection in aircraft structures. *Review Literature And Arts Of The Americas*. http://doi.org/10.1117/12.818114

Simulia. (2012). Getting Started with Abaqus: Interactive Edition. *Getting Started with Abaqus: Interactive Edition*, 4.50-4.54. Retrieved from http://www.maths.cam.ac.uk/computing/software/abaqus_docs/docs/v6.12/pdf_books

/GET_STARTED.pdf

Smith, W. F., & Hashemi, J. (2001). *Foundations of Material Science and Engineering* (5th ed.). New York: McGraw-Hill.

Styles, M., Compston, P., & Kalyanasundaram, S. (2007). The effect of core thickness on the flexural behaviour of aluminium foam sandwich structures. *Composite Structures*, *80*, 532–538. http://doi.org/10.1016/j.compstruct.2006.07.002

Thill, C., Etches, J. A., Bond, I. P., Potter, K. D., Weaver, P. M., & Wisnom, M. R. (2010). Investigation of trapezoidal corrugated aramid/epoxy laminates under large tensile displacements transverse to the corrugation direction. *Composites Part A: Applied Science and Manufacturing*, *41*(1), 168–176. http://doi.org/10.1016/j.compositesa.2009.10.004

Tian, Y. S., & Lu, T. J. (2005). Optimal design of compression corrugated panels. *Thin-Walled Structures*, *43*(3), 477–498. http://doi.org/10.1016/j.tws.2004.07.014

Vaidya, S., Zhang, L., Maddala, D., Hebert, R., Wright, J. T., Shukla, A., & Kim, J. (2015). Quasi-static response of sandwich steel beams with corrugated cores. *Engineering Structures*, *97*, 80–89. http://doi.org/10.1016/j.engstruct.2015.04.009

Xu, G., Yang, F., Zeng, T., Cheng, S., & Wang, Z. (2016). Bending behavior of graded corrugated truss core composite sandwich beams. *Composite Structures*, *138*, 342–351. http://doi.org/10.1016/j.compstruct.2015.11.057

Yan, L. L., Han, B., Yu, B., Chen, C. Q., Zhang, Q. C., & Lu, T. J. (2014). Three-point bending of sandwich beams with aluminum foam-filled corrugated cores, *60*, 510–519. http://doi.org/10.1016/j.matdes.2014.04.014

Yan, L. L., Yu, B., Han, B., Chen, C. Q., Zhang, Q. C., & Lu, T. J. (2013). Compressive strength and energy absorption of sandwich panels with aluminum foam-filled corrugated cores, *86*, 142–148. http://doi.org/10.1016/j.compscitech.2013.07.011

Yazici, M., Wright, J., Bertin, D., & Shukla, A. (2014). Experimental and numerical study of foam filled corrugated core steel sandwich structures subjected to blast loading. *Composite Structures*, *110*, 98–109. http://doi.org/10.1016/j.compstruct.2013.11.016

Yokozeki, T., Takeda, S. ichi, Ogasawara, T., & Ishikawa, T. (2006). Mechanical properties of corrugated composites for candidate materials of flexible wing structures. *Composites Part A: Applied Science and Manufacturing*, *37*, 1578–1586. http://doi.org/10.1016/j.compositesa.2005.10.015

Zhang, P., Liu, J., Cheng, Y., Hou, H., Wang, C., & Li, Y. (2015). Dynamic response of metallic trapezoidal corrugated-core sandwich panels subjected to air blast loading – An experimental study. *Journal of Materials & Design*, *65*, 221–230. http://doi.org/10.1016/j.matdes.2014.08.071

Zhao, H., Elnasri, I., & Girard, Y. (2007). Perforation of aluminium foam core sandwich panels under impact loading-An experimental study. *International Journal of Impact Engineering*, *34*, 1246–1257. http://doi.org/10.1016/j.ijimpeng.2006.06.011